Korean J. Chem. Eng., 32(8), 1455-1476 (2015)
DOI: 10.1007/s11814-015-0104-0

pISSN: 0256-1115
eISSN: 1975-7220

REVIEW PAPER

Reviews on drag reducing polymers

Angnes Ngieng Tze Tiong†, Perumal Kumar, and Agus Saptoro

Department of Chemical Engineering, Curtin University Sarawak Campus, CDT 250, 98009 Miri, Sarawak, Malaysia
(*Received 31 October 2014 • accepted 16 May 2015*)

Abstract−Polymers are effective drag reducers owing to their ability to suppress the formation of turbulent eddies at low concentrations. Existing drag reduction methods can be generally classified into additive and non-additive techniques. The polymer additive based method is categorized under additive techniques. Other drag reducing additives are fibers and surfactants. Non-additive techniques are associated with the applications of different types of surfaces: riblets, dimples, oscillating walls, compliant surfaces and microbubbles. This review focuses on experimental and computational fluid dynamics (CFD) modeling studies on polymer-induced drag reduction in turbulent regimes. Other drag reduction methods are briefly addressed and compared to polymer-induced drag reduction. This paper also reports on the effects of polymer additives on the heat transfer performances in laminar regime. Knowledge gaps and potential research areas are identified. It is envisaged that polymer additives may be a promising solution in addressing the current limitations of nanofluid heat transfer applications.

Keywords: Drag Reduction, Polymer Additives, Computational Fluid Dynamics (CFD), Heat Transfer, Nanofluid

INTRODUCTION

Studies on drag reduction (DR) techniques have become very popular over the past few decades, as they improve the mechanical efficiency of flow systems. These techniques have found extensive use in applications such as the transportation of crude oil, suspensions and slurries, district heating and cooling, oil well fracturing operations, hydro-transport of solids and biomedical fields [1].

Toms [2] indicated that DR could be achieved by using polymer additives and concluded that different types of polymers could serve as effective drag reducers. Polymer was first commercially used in 1979 as a drag reducer in a 48 inch diameter and 800 mile long Trans Alaska crude oil pipeline from North to South Alaska [3]. Since then, polymer additives have been acknowledged for their DR ability. DR of up to 80% can be attained by adding only a few parts per million of polymer.

This paper has five main sections: (1) Polymer-induced DR, (2) Classification of DR methods, (3) Laminar heat transfer enhancement by polymer additives, (4) Potential research area: Addition of drag reducing additives to nanofluid (Drag reducing nanofluid), (5) Knowledge gap and future research directions. Section 1 aims to provide an overview of experimental and CFD modeling studies related to polymer-induced DR in turbulent flow. In section 2, different types of existing DR methods are briefly discussed and compared to polymer-induced DR. The associated heat transfer performance of polymer additives in laminar flow is also discussed in section 3, followed by potential research areas of drag reducing nanofluid in section 4. Finally, knowledge gap, future research directions and recommendations are outlined in section 5.

†To whom correspondence should be addressed.
E-mail: angnesnt@hotmail.com, angnes@postgrad.curtin.edu.my

POLYMER-INDUCED DR

As mentioned, Toms [2] was the first to identify polymers as effective drag reducing additives. He observed that the addition of polymethyl methacrylate to monochlorobenzene could reduce turbulent skin friction drag by 80%. Liaw et al. [4] investigated the effect of molecular characteristics of different polymers on DR. It was concluded that for effective DR to occur, polymers must exceed a minimum chain size. Drag reducing polymers are normally long-chain, high-molecular weight (ranging from 1 to 10 millions) polymers such as polyethylene oxide (PEO) and polyacrylamide (PAA) [5-7]. They also exhibit non-Newtonian and viscoelastic behaviors [8-11]. To date, polymer additives are the most studied among all drag reducing methods, because at a low quantity, a significantly large DR can be attained.

Parameters influencing the performances of drag reducing polymers include flow rate, injection point, channel size, geometry, surface roughness, molecular weight, chain flexibility, structure, concentration, solvent, salt content, pH, and temperature [12-16]. Generally, DR increases with increasing polymer concentration, polymer molecular weight, Reynolds number, and flow rate. However, it is inversely proportional to the pipe diameter [13,17-20].

According to Abubakar et al. [15], polymer additives could suppress the turbulent burst formation in buffer layers, which in turn restrain the development and distribution of turbulent eddies, as shown in Fig. 1. After drag is reduced, less energy is wasted for turbulent random motions and more energy can be used to move the fluid along the pipeline. Lumley [21] postulated that polymer-induced DR occurred due to the increased extensional viscosity during the stretching of randomly coiled polymers under fluctuating shear rate. Extensional viscosity, also known as elongational viscosity, is a term used for viscosity, when the extensional stress is applied [22]. Higher extensional viscosity dampened the turbulent energy in the

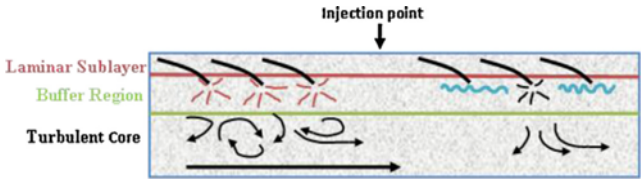

Fig. 1. Schematic of pipeline turbulent flow regions [15].

buffer layers, and thus resulted in lower turbulent energy dissipation and friction. DR only took place if the relaxation time of polymeric solution was greater than the characteristic time of the turbulent flow. Relaxation time is the time required for polymer chain to return to equilibrium in response to a disturbance [21]. Dimitropoulos et al. [23] agreed with Lumley [21] on his postulation. Similarly, from their experiments, Bonn et al. [24] also showed that polymer-induced DR was attributed to the elongational viscosity, in which DR increased with the increasing elongational viscosity.

To study the effect of elastic polymer stresses on DR, Gillissen [25] performed direct numerical simulations of turbulent channel flow, using two different equations to represent rigid and flexible polymers. Elastic polymer stresses were attributed to the coiling and stretching of the flexible polymers. The results demonstrated that polymer elasticity played a minor role in DR mechanism. Polymer-induced DR was due to viscous polymer stresses introduced by the extended polymers. A similar conclusion was drawn by Toonder et al. [26]. In addition, Toonder et al. [26] stated that DR efficacy decreased with the increasing polymer flexibility. They proposed that the onset of DR was determined by the elastic properties of polymer before the polymer became extended. After the extension, the viscous effect caused DR and polymer elasticity to have an adverse effect on DR.

Nevertheless, Kwack and Hartnett [19] and Kwack et al. [18] disagreed and proposed that the DR of polymeric solution originated from the elasticity properties of the macromolecules of polymers. Furthermore, it was also suggested that the DR was related to the thickened viscous layers near to the duct wall [6].

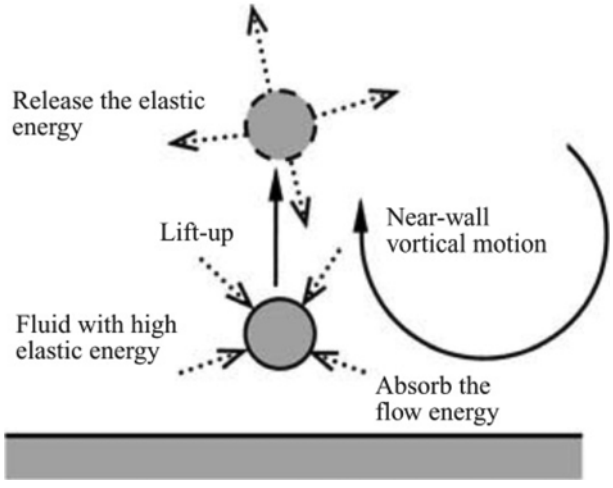

Fig. 2. Schematic representation of DR mechanism proposed by Min et al. [27].

Min et al. [27] hypothesized that polymer additives absorbed the kinetic energy near the wall region and this absorbed energy was transformed into elastic energy. When the relaxation time was long enough, this elastic energy would be lifted up by near-wall vortical motion and dissipated into buffer or log layers as illustrated by Fig. 2. The near-wall turbulence was weakened, and thus led to DR. From different theoretical mechanisms of polymer-induced turbulent DR as proposed by different researchers above, it can be highlighted that the mechanisms of polymer-induced DR still remain unclear.

1. Experimental Works Related to Polymer-induced Turbulent DR

Most research on polymer additives has been in the turbulent regime. Tung et al. [28] experimentally studied the friction factor for 1,500, 2,000 and 2,500 ppm of PAA solutions, and reported that the friction factor was lower than the maximum DR asymptote as proposed by Virk [29]. McComb and Rabie [13] discovered that the addition of 10 to 100 ppm PAA and PEO in water reduced pressure loss in the range of 60-70%. They deduced that DR was related to the interactions of polymer additives with the near-wall turbulence.

Kim et al. [20] measured the DR in polymer added turbulent flow to provide some experimental data for application of polymer additives in a nuclear district heating system. From all the molecular weight and concentration ranges tested, a DR of greater than 20% could be obtained with the polymer solution. It was found that 20 ppm PEO with molecular weight of 4×10^6 achieved the maximum DR of 50%. Virk et al. [12] examined the effect of concentration on DR in PEO-water pipe flow. They noted that there was an optimum concentration for maximum DR, and beyond this, the viscosity increment had significant negative impacts on the DR phenomena. A similar observation was also made by Kim et al. [20].

Nevertheless, some of the above mentioned researchers [12,13, 20,28] did not investigate the effect of polymer additives on the heat transfer performance. Kwack et al. [18] stated that 5 ppm of PAA could reduce the friction and heat transfer up to around 30% and 46%, respectively. Kwack and Hartnett [19] carried out turbulent heat transfer studies of polymer solution in circular pipe flow under constant heat flux condition. It was found that at higher concentrations, where there was substantial DR, the dimensionless heat transfer coefficient drastically decreased compared to the friction factor at the same Reynolds and Prandtl number. Gupta et al. [11] measured the heat transfer coefficient for 0.05% and 0.45% PAA in water. The results showed that both 0.05% and 0.45% polymer solutions could reduce drag up to 44% and 36%, respectively, at a flow rate of 200 pound per minute. DR was observed to coexist with the reduction in heat transfer rate. The maximum heat transfer rate reduction for 0.05% and 0.45% PAA solutions were found to be 62% and 90%, respectively. This suggests that the DR was caused by the suppression of turbulence.

Similarly, Poreh and Paz [30] reported that the flow of a diluted polymeric solution (from 10 to 1,000 ppm, Pr>1) in circular ducts, the reduction in Nusselt numbers was larger than the friction factor decrement, especially at high Reynolds numbers. Comparable findings were also made by Gupta et al. [11], Kwack et al. [18], Kwack and Hartnett [19], Hartnett and Kwack [31], as well as Debrule and Sabersky [32]. For heat transfer reduction, it is plausible that the

presence of polymer additives thickened the near-wall elastic buffer layers, which increased the thermal resistance between the wall and bulk fluid, resulting in a lower heat transfer rate [33-35]. Debrule and Sabersky [32] carried out a series of experiments to determine the heat transfer and friction coefficients for smooth and rough circular tubes, by using PEO in water. For rough circular tubes, drastic reduction in friction and heat transfer coefficient was by a factor of 6 and 10, respectively, while for smooth tubes, the friction coefficient was reduced by a factor of 3, and heat transfer by a factor of 5. Their results also indicated that the performance of polymers decreased with the increasing Reynolds number, due to its degradation. Lower concentrations of polymer solutions, which were exposed to higher temperatures, were also more susceptible to structure degradation.

Toh and Ghajar [36] conducted a study in the thermal entrance region of turbulent pipe flow, by using two different types of PAA solutions (separan AP-273 and AP-30) under constant wall heat flux condition. PAA (separan AP-273) was found to be more effective than PAA (separan AP-30), owing to its higher molecular weight and elasticity. For example, at Reynolds number of 15000, the rates of heat transfer reduction caused by the addition of 200 ppm of separan AP-273, and separan AP-30 were 85% and 57%, respectively. Results demonstrated that the Nusselt number decreased with the increasing polymer concentrations, until a certain asymptotic limit. Further increment beyond the asymptotic limit had no effect on heat transfer. In addition, the results showed that the reduction of heat transfer was more significant in smaller pipes when compared to larger ones. For example, at the dimensionless axial distance of 300, PAA (separan AP-30) reduced heat transfer up to 61% in a 1.11 cm pipe section, while heat transfer reduction was only 41% in a 1.88 cm pipe section. This was attributed to the effect of polymers on near-wall boundary layers. The wall boundary layers contributed to a larger amount of the total flow in a smaller pipe, so the influence of polymers on it was more considerable.

Non-circular ducts, especially rectangular ducts, have been used for the development of liquid cooling modules for electronic packaging and other industrial applications. Thus, this type of geometry is becoming of great interest to research [37-40]. However, studies on the friction factor and heat transfer characteristics of turbulent non-circular flow are comparatively scarce [16]. Escudier and Smith [41] carried out DR studies in a square duct for fully developed flow region using an aqueous solution of 0.1% carboxymethylcellulose, combined with 0.1% xanthan gum (CMC/XG), and 0.125% aqueous solution of PAA separately. PAA, which is more elastic compared to CMC/XG, produced higher DR of 77%, while CMC/XG only achieved a DR of 65% in turbulent flow.

Kostic and Hartnett [42] performed heat transfer and friction factor studies in a 2 : 1 rectangular duct using aqueous PAA solution. Similar to circular turbulent flow, in a rectangular duct, drag was greatly reduced, along with heat transfer reduction, by the addition of PAA additives to water. Friction factor and heat transfer decreased with the increment of polymer concentration, until an asymptotic value, and any further increment of polymer concentration had no impact on heat transfer and friction drag. The maximum DR asymptote and heat transfer asymptote were reached at PAA concentrations of 100 and 1,000 ppm, respectively. It was noted that the asymptotic value for friction factor was much smaller compared to the asymptotic value for heat transfer. Moreover, this also suggests that the friction factor and dimensionless heat transfer coefficient can be predicted using the available correlations for the turbulent flow of PAA solution in circular ducts.

Polymer additives are also used to reduce drag in open turbulent flow. Yang et al. [43] carried out turbulent DR experiment using PEO, in a rotating disk apparatus (RDA). The RDA can be used to describe the external flow, which includes the flow over flat plates and the flow around submerged objects. They found that the maximum DR achievable by PEO in the RDA was 22.7%. Kim et al. [44] simulated external flow using a high-precision RDA to study the polymer-induced DR. For PEO and XG tested, DR increased with the increasing Reynolds number. Time-dependent DR was also investigated and the results showed a decrement in DR due to polymer degradation. Also, the DR of polymeric solutions was found to be lower at higher temperature.

Choi et al. [45] also examined turbulent DR in RDA using an oil-soluble polymer, polyisobutylene (PIB). They reported that polymer-solvent interactions played an important role in DR. In their studies, cyclohexane and xylene were employed as solvents. When 2.1×10^6 g/mol PIB was used, the maximum DR achieved by PIB-cyclohexane and PIB-xylene systems were 23.9% and 31.8%, respectively.

The effect of different solvents (benzene, chloroform and toluene) on turbulent DR and mechanical degradation of polystyrene using RDA was investigated by Kim et al. [46]. DR efficiency was observed to decrease as a function of time, due to polymer degradation. Additionally, their results indicated that the degree of polymer degradation was greatly influenced by the solubility parameter of the solvents.

A study similar to Choi et al. [45] was done by Lim et al. [47]. However, they employed monodisperse and high molecular weight deoxyribonucleic acid (DNA). The DR efficiency of DNA was also compared to flexible long chain PAA. A DR up to 20% was attained by adding 2.70 ppm of DNA, and DR increased with the increasing DNA concentration. Nevertheless, turbulent DR efficiency declined within a few minutes after an injection of polymer solution, as a result of mechanical degradation. After reaching a limiting value, the DR efficiency was maintained for an extended period of time. Conversely, the DR efficiency of PAA drastically dropped within the first few minutes, and no further DR was reported thereafter. Although the DNA rapidly degraded initially, its residual DR ability was maintained due to the midpoint scission of its molecules. Lim et al. [48] further examined the effect of DNA structural arrangement, or conformation, on the DR efficiency, by adding spermidine (SPD) as a condensing agent of DNA to the turbulent flow. An abrupt reduction in the DR efficiency was found after the SPD injection. They believed that the mechanical degradation was not the reason for the DR efficiency reduction. This reduction was most likely caused by the gradual changes in DNA conformation under turbulent conditions in the presence of SPD. The DNA was presumed to have been transformed from coil to globular form, which did not promote DR. Lim et al. [48] had the same opinion as Kim et al. [49], that changes in polymer conformation altered the behaviors of the turbulent flow.

Sohn et al. [50] conducted experiments in a rotating disk flow to study DR of XG. From these experiments, XG was found to be an effective drag reducer for high temperature applications. XG demonstrated a higher DR at 50-60 °C compared to the DR obtained at room temperature. This was because as at high temperature, XG transformed from a helical structure to individual coil, which was a better polymer conformation for DR. Moreover, DR achieved by the addition of XG increased with its concentration until maximum DR was attained.

Kim et al. [51] investigated the turbulent DR characteristic of polysaccharide guar gum with RDA, and then compared the results with those obtained using PEO. Although, PEO, a synthetic water-soluble drag reducing polymer, was more effective for DR, it degraded faster when compared to guar gum. DR efficiency of the PEO solution dropped more than 10% after the first 10 minutes in a rotating disk flow, while guar gum exhibited significant resistance to mechanical stress.

A mixture of polymer and surfactant is also believed to be a good drag reducer. Kim et al. [49] further explored the effect of pH and surfactant on the DR efficiency of polymer additives in open turbulent flow by using RDA. An illustration of the conformational variation of PAA molecular at different pH levels is given in Fig. 3. Their results showed that at pH 11, the DR efficiency was higher

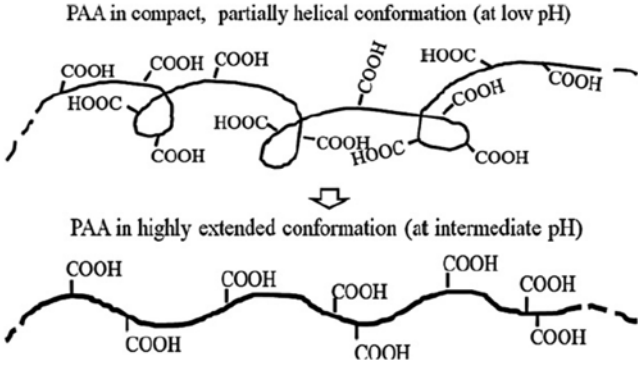

Fig. 3. Illustration of PAA conformation at different pH levels [49].

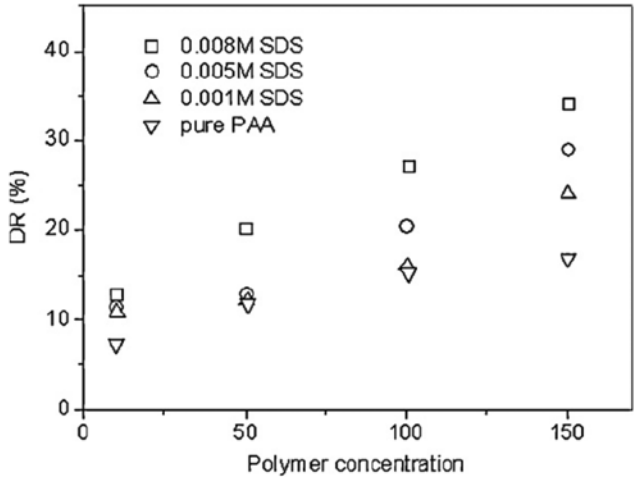

Fig. 4. DR as a function of polymer concentration (pH=4) with various sodium dodecyl sulfate (SDS) concentration [49].

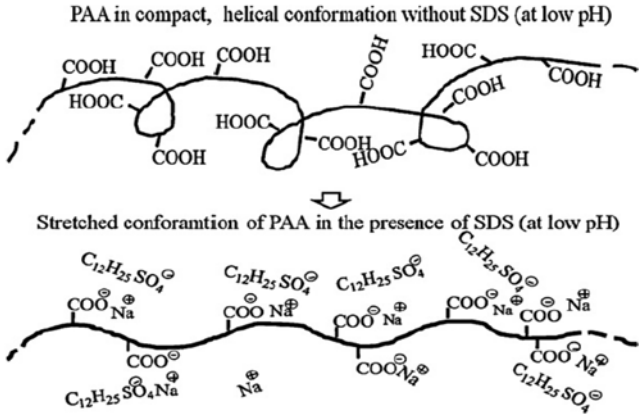

Fig. 5. Illustration of PAA conformation after adding surfactant SDS [49].

compared to that at pH of 4 and 7. Therefore, they postulated that a highly extended polymer conformation was more favorable for DR in turbulent flow. DR increased with the increasing surfactant concentration, as shown in Fig. 4. As presented in Fig. 5, interaction between surfactant and polymer chains enhanced the bonding force of polymer molecules, and stretched the polymer chains, thus leading to higher DR, especially at lower pH levels. From the work done by Kim et al. [49], it can be deduced that a mixture of polymer and surfactant serves as a better drag reducer compared to a pure polymer solution.

Matras et al. [52] indicated that the mixed PEO and cetyltrimethyl ammonium bromide (CTAB) solution may serve as a drag reducer in pipe flow. When polymer and surfactant were mixed in water, aggregates were formed in which polymer film encircles the micelle. This mixed polymer-surfactant solution showed a higher DR than pure polymer and surfactant solutions. Moreover, this mixed system resisted shear rate better than that of individual substances alone, as it took longer for the mixed solution to degrade. The damaged aggregates were partly self-repaired.

In different studies, Mohsenipour and Pal [53] examined the turbulent DR behavior of mixed nonionic polymer and cationic surfactant solution. PEO and octadecyltrimethyl ammonium chloride (OTAC) were used in their experiments. Experimental results showed that this mixed polymer-surfactant solution gave a higher DR when compared to a pure polymer or pure surfactant solution. This synergistic effect was also found to be more significant at low polymer concentrations and high surfactant concentrations. The rates of DR achieved by the mixed polymer-surfactant solution were 58% and 35% higher as compared to the pure surfactant and pure polymer solutions, respectively. It was hypothesized that the DR was caused by the new three-dimensional microstructure. This microstructure was formed when the micelle of the surfactant was attached to the polymer chain and it could suppress the turbulence eddies.

2. CFD Studies Related to Polymer-induced Turbulent DR

Numerical investigations have also been conducted by researchers to study polymer-induced DR. Dimitropoulos et al. [23] utilized the FENE-P model and Giesekus model in their numerical simulations of turbulent channel flow of a polymer solution, and

Table 1. Summary of CFD studies related to polymeric solution

Author	Geometry	Flow regime	Types of polymer used	Model used for simulation	Remarks
Shin and Cho [38]	2 : 1 Rectangular duct	Laminar - With heat transfer - Constant axial heat flux - Constant peripheral wall temperature (top-wall heated with all others adiabatic)	1,000 ppm PAA (separan AP-273)	Carreau model with fluid property of temperature dependent and shear thinning viscosity	• Compared to constant property, using temperature dependent and shear thinning viscosity model could better predict the heat transfer performance of PAA solution. • The Nusselt number was enhanced by 70-300% compared to the one using constant fluid property. • Heat transfer enhancement was due to the increasing of near-wall velocity gradient from the combined effect of temperature dependent and shear thinning viscosity.
Naccache and Mendes [59]	Rectangular duct (*with duct aspect ratio of 1, 2 & 4*)	Laminar - With heat transfer - Top and bottom wall under constant heating and side walls adiabatic	Non-Newtonian viscoelastic solution (*the type of non-Newtonian solution is not mentioned*)	Criminale-Ericksen-Filbey (CEF)	• The presence of secondary flow did not have any effect on friction factor. • Secondary flow enhanced the Nusselt number of non-Newtonian solution up three times larger than relative Newtonian flow. Effect of secondary flow on heat transfer enhancement was dominant compared to impact of shear thinning viscosity. • For maximum heat transfer performance, there existed an optimum combination of aspect ratio and Reynolds number.
Dimitropoulos et al. [23]	Channel	Turbulent - Without heat transfer - Constant pressure gradient	Dilute and concentration polymer solution	FENE-P & Giesekus model	• DR was attributed to the extensional viscosity of the polymer. • When the extensibility viscosity of the polymer increased, triple increment in DR was observed.
Min et al. [27]	Channel	Turbulent - Without heat transfer - Constant mass flow across channel	Polymer solution	Oldroyd-B model	• Polymer absorbed the turbulent kinetic energy near the wall, transformed them to elastic energy and transported them to buffer layers. This intervened turbulent energy transfer and led to DR. • Relaxation time must be long enough for DR to occur as dissipation of elastic energy near wall to buffer layers needed time.
Ptasinski et al. [54]	Channel	Turbulent - Without heat transfer - Constant pressure drop	Polymer solution	FENE-P model	• Stretching of polymers was necessary for DR. • During DR, velocity fluctuations decreased and moved away from wall. • FENE-P model could not fully represent the rheological behavior of polymer solution.
Dhotre et al. [56]	Pipe	Turbulent - Without heat transfer	PAA, XG, CMC, and blend of XG/CMC solution	Low Reynolds number k-ε model	• Low Reynolds number k-ε model could be used to cater the liquid and turbulent velocities for drag reducing fluids quite accurately.

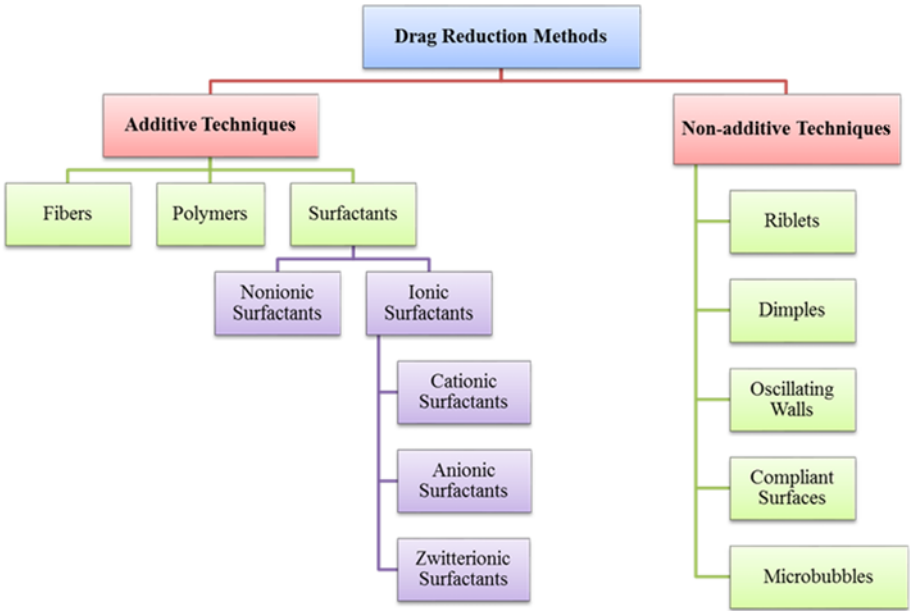

Fig. 6. Classification of DR methods.

compared both of the results obtained. The results demonstrated that the onset of DR took place at a certain critical Weissenberg number. Both the Giesekus model and the FENE-P simulations reached the same conclusion that the DR was due to the extensional viscosity.

Min et al. [27] employed a numerical model to simulate and study the DR mechanism of polymer additives in turbulent channel flow. An Oldroyd-B model (linear Hookean dumbbells) was used to represent the linear elastic behaviors of the polymer additives. Min et al. [27] pointed out that there was a threshold of the Weissenberg number for DR to occur. For a Reynolds number of 15000, and the Weissenberg number of 2, DR up to 28% could be obtained.

Ptasinski et al. [54] also used the FENE-P model to observe the elastic behavior of polymers in turbulent channel flow. It was observed that with increasing DR, the buffer layers were considerably thickened. Moreover, spanwise and wall-normal velocity fluctuations were shifted away from the wall monotonically during higher DR.

In contrast, Lagrangian simulations were recommended by Terrapon [55] to investigate the DR of a dilute polymer solution in turbulent channel flow. The Lagrangian approach has the ability to track a large amount of turbulent polymer molecules and compute polymer stress along the flow directions. Therefore, the dynamics of a single polymer molecule could be described by the simulations. Terrapon [55] proposed a novel numerical technique based on the Lagrangian approach to model and simulate the DR. In another study, Dhotre et al. [56] used CFD simulation to examine the flow pattern of drag reducing fluids in the turbulent pipe flow. They concluded that drag reducing fluids could be modeled using the low Reynolds number k-ε model. The low Reynolds number k-ε model utilized the non-linear viscosity and damping function to take the near-wall effects into account. It was found that the simulation results on axial velocity and kinetic energy were in agreement with the experimental profiles of Escudier et al. [57] and Presti [58].

The CFD related studies are summarized in Table 1. From Table 1, there is an absence of proper constitutive equations for solving polymers related to the CFD studies. Different researchers use different models to represent the behavior of polymers in CFD.

CLASSIFICATION OF DR METHODS

DR methods can be broadly classified into additive and non-additive techniques. Polymers are one of the additive DR techniques. The major non-additive and additive DR methods are shown in Fig. 6.

1. Riblets

Riblets are longitudinal microgrooves attached to a surface that resemble the scale pattern of a shark. When a shark is swimming,

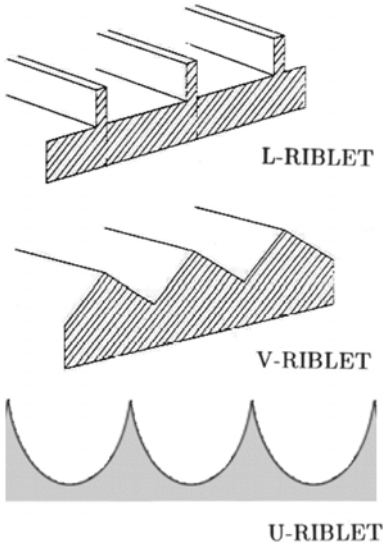

Fig. 7. V, U and L-shaped riblets [62,63].

its skin exhibits riblet structures that align to the flow direction to reduce skin drag [60]. In addition, riblets provide larger surface area, thus promoting higher momentum and heat transfer rate [61]. Riblets have different shapes, but the most common designs are V-shaped (triangular), U-shaped (scalloped) and L-groove (rectangular) riblets as shown in Fig. 7.

Riblets were first used at NASA Langley Research Centre to reduce the friction of aircraft airflows [64]. Walsh [65] reported that the presence of riblets reduced a small amount of drag and this conclusion was in agreement with the preliminary results of Liu et al. [66] who used a longitudinal rectangular ribbed surface. This has led to further research on the effectiveness of riblets as drag reducer.

Choi et al. [67] studied numerically the effect of riblets in a fully developed laminar channel flow by solving the Poisson equation. They used a W-type multigrid cycle for the spanwise direction and tridiagonal solver for the normal direction. Their results showed that drag was not reduced in the laminar channel flow. Chu and Karniadakis [68] carried out direct numerical simulations over the riblet-mounted surfaces, covering laminar, transitional and turbulent regimes with the Reynolds number ranging from 500 to 3500. The riblets were simulated in the lower wall of the channel using the spectral element-Fourier method. Their results were in agreement with Choi et al. [67] that no DR was found for the laminar regime. DR was only reported for transitional and turbulent regimes.

Many studies have shown that riblets are capable of reducing the turbulence intensity up to 6-10% [68-72]. In spite of this, there is no general consensus on the mechanisms underlying the DR phenomena of riblets. Kwing-So Choi [69] and Warsop [70] suggested that riblets serve as fences in restricting the stream-wise movement of longitudinal vortices, leading to premature occurrence of burst with reduced duration and turbulence intensity. Haecheon Choi and his co-workers [71] proposed that riblets reduced drag by limiting the streamwise vortices above the wetted riblet surface. Another theory claimed that DR by riblets was achieved by viscous interaction between the longitudinal vortices and small eddies near the riblets peaks, which in turn produced secondary vortices that dampened the longitudinal vortices and maintained low-speed flow through riblet valleys [73].

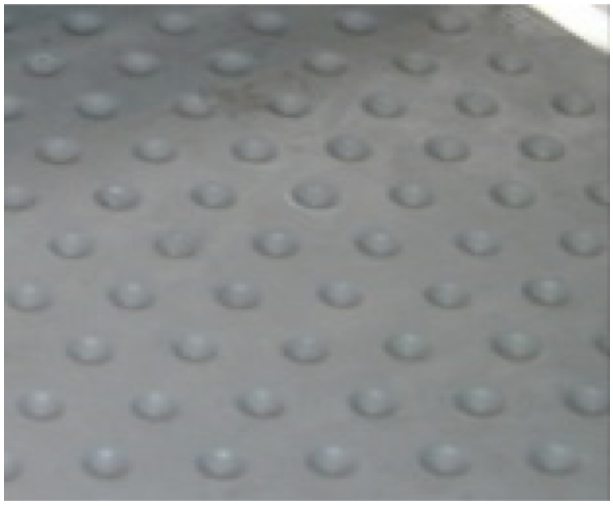

Fig. 8. A dimpled surface [77].

2. Dimples

Dimples are regular arrangements of discrete indentations milled onto a wall surface, primarily used for heat transfer enhancement (Fig. 8). Alekseev et al. [74] experimentally observed that besides improving heat transfer, dimples could reduce turbulent skin-friction up to 20%. However, the underlying mechanisms of DR are still unexplainable. Most common use of dimples for DR can be seen in golf balls [75,76] where dimples are able to help reducing drag caused by the air resistance acting against the flow direction. Dimples also increase the lift force in the golf balls.

Lienhart et al. [78] did experiments and direct numerical simulations for turbulent flow over dimpled surfaces and reported improved heat transfer performance without any significant effect on drag. Whereas, Kim et al. [79] reported improvement in both heat transfer and drag. They numerically estimated the friction loss and heat transfer of turbulent flow in a cooling channel with staggered elliptic dimples. The optimized dimple design was found to increase heat transfer rate by 32.8% and decrease the frictional loss by 34.6%. Silva et al. [80] investigated dimple performance experimentally and numerically, for constant heat flux boundary condition. Nusselt number of dimpled surfaces was higher compared to a flat surface. Moreover, friction also increased with the increasing Reynolds number. Overall performance of dimples was generally good at low Reynolds number, as friction was relatively small. Hence, the uses of dimples are suggested only for laminar flow application such as in microelectronic cooling. In addition, Burgess et al. [81] found experimentally that dimples enhanced heat transfer performance; however, friction factor ratios increased with the increasing Reynolds number. When Reynolds number increased from 12000 to 70000, the friction factor ratio also increased from 1.6 to 2.6. Silva et al. [80] and Burgess et al. [81] opined that the use of dimples increased pressure drop and these results are contradictory to that reported by Kim et al. [79].

These inconsistent results reported in literature may be attributed to the differences in the geometry of dimples (shapes, depth and spacing) as studied, flow type (internal or external), flow regime (Reynolds number range), measurement techniques and result analysis methods. For example, Samad et al. [82] applied the same methods used by Kim et al. [79] in their multi-objective optimization. Their results showed that the heat transfer performance and pressure drop of the flow across dimples were affected by dimple depth and spacing. Heat transfer and pressure drop increased with the increase of dimple depth, but decreased with the increase of dimple spacing.

Veldhuis and Vervoort [77] analyzed the DR capabilities of dimples, using experiments and large eddy simulation (LES). Experimental results pointed out that the shallow dimple (0.343 mm≤depth ≤0.5 mm) reduced drag, while the deep dimples (1.5 mm≤depth≤ 3.5 mm) increased drag. For the shallow dimples, 20% DR was reported at low flow velocities. Dimples with intermediate depth reduced drag only at low flow velocities. In contrast, their simulation results showed that drag increased for both shallow and deep dimples.

3. Oscillating Walls

Oscillating walls is a technique in which one or two walls are

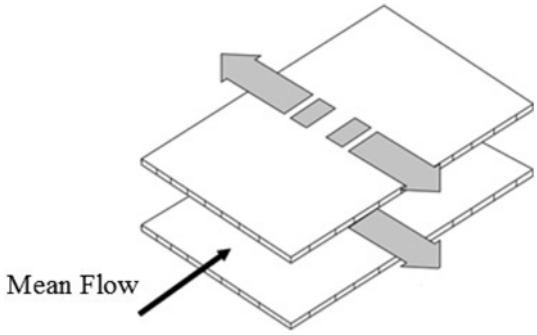

Fig. 9. Schematic of spanwise oscillation for channel flow [90].

subjected to motor-driven forced spanwise or streamwise oscillation [61]. Most studies are conducted on spanwise oscillating walls as shown in Fig. 9. Oscillating walls were developed based on the concept that the turbulent phenomenon can be suppressed when a sudden spanwise pressure gradient is applied on the near-wall turbulent flow field. There is a common agreement that wall oscillation at suitable velocity, frequency and amplitude promotes DR. This is because the oscillation alters the near-wall boundary layers, and thus reduces the turbulence intensity [83-89].

The first spanwise wall oscillation was studied by Jung et al. [91]. They used direct numerical simulation to investigate the spanwise oscillation of wall-bound turbulent flow and reported a DR of 10 to 40%. The maximum drop in turbulence intensity was found to be 35%. Fang et al. [84] simulated the turbulent channel flow with spanwise wall oscillation and modeled it using LES to inspect the effects of the oscillating walls. It was found that a maximum DR of 46% could be attained.

Baron and Quadrio [85] in their numerical simulations of Navier-Stokes equations for a plane channel flow with spanwise wall oscillation, obtained up to 40% turbulent DR. They also claimed that the energy saved in the reduction of friction could be counter-balanced by the power supplied to sustain the oscillating walls, particularly at low wall-oscillation amplitude and velocity. Ten percent net power saving was observed. Quadrio and Ricco [92] also found that a maximum net energy saving of approximately 7.3-10%, along with 44.7% maximum DR, could be achieved using oscillating walls.

Laadhari et al. [86] experimentally investigated the turbulence boundary layers on a flat plate subjected to spanwise wall oscillation and suggested that skin friction drag could be reduced using oscillating walls. This suggestion was later proven by Choi et al. [87], Choi and Clayton [88], and Choi [89] in their experiments. Their experimental results showed that 45% skin friction reduction could be attainable at the downstream of spanwise wall oscillation. This result agreed closely with those obtained from simulations [84,85,91,92]. These researchers [86-89] agreed that DR is driven by the spanwise vorticity developed via wall oscillation. This vorticity reduced the near-wall mean velocity gradient and aligned the vortices, leading to a drop in turbulent fluctuations.

Choi and Graham [93] experimentally studied DR in a turbulent pipe flow by imposing circular-wall oscillation to a section of the pipe. The friction factor of the pipe was reduced by 25%. The DR achieved in pipe flow was much smaller than the DR obtained

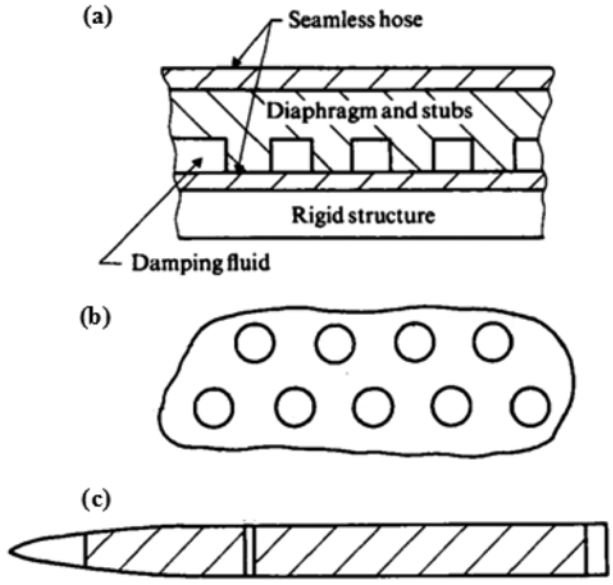

Fig. 10. Kramer's coatings and model: (a) cross section, (b) cut through stubs, (c) model: shaded regions were coated [94, 99].

in their other research work [87-89] on external flow. It was postulated that DR in pipe flow is the result of realignment of longitudinal vortices in circumferential direction (direction of the oscillating wall).

4. Compliant Surfaces

Similar to riblets, the idea of compliant surfaces also comes from the turbulence control technique of marine organisms. Kramer [94] first observed that dolphins can swim at high speeds because of their flexible skin, which has a drag resistant nature. He discovered that 60% DR could be achieved by the compliant coatings (Fig. 10) modeled after dolphins' skin. DR was achieved by delaying transition to turbulence. However, the 60% DR obtained by Kramer [94] could not be reproduced by other researchers [95-98].

Benjamin [100], Betchov [101], and Landahl [102] performed theoretical studies on compliant coatings and reported that DR by transition to turbulence postponement was possible. The early studies by these researchers [100-102] focused on DR by delaying transition to turbulence in laminar boundary layer, but not on reducing turbulent skin friction in turbulent boundary layer using compliant surfaces.

Carpenter and Garrad [99] analyzed experiments by Kramer [94] and other researchers [95-98], in order to check the DR capability of Kramer's coatings. Carpenter and Garrad [99] claimed that Kramer's coatings were only capable of delaying transition to turbulence. The reason that Kramer's coatings did not perform well for these researchers [95-98] might be the differences in the experimental conditions. It was difficult to make compliant surfaces, as the material properties were sensitive to changes. Undesirable factors like poor pressure gradient, or problems in making joints between compliant and rigid surfaces, could affect the performance of the coatings. Moreover, Kramer's coatings were also not flexible enough to be used for higher Reynolds number flows. Therefore, the results from these experiments [95-98] were inconclusive in

proving that DR achieved by Kramer [94] is irreproducible.

In 1991, Kulik et al. [103] used the optimum compliant surfaces produced by Semenov [104] in their experimental work. They reported a successful turbulent DR in a lake and their experimental results were validated by Choi et al. [105]. Choi et al. [105] were also able to demonstrate that compliant surfaces could indeed reduce skin friction for turbulent boundary layers. Skin-friction and near-wall pressure fluctuations were reduced to around 7% and 19%, respectively, in downstream, where the compliant surfaces were fixed. Turbulence intensity was also reduced up to 5%. In addition, the thickness of the viscous sub-layers increased along with turbulent DR.

Endo and Himeno [106] performed direct numerical simulation of a turbulent duct flow over compliant surfaces. Two to −3% average and 7% maximum DR were achieved with weak wall displacement of the compliant surfaces. The DR results obtained by Choi et al. [105] through experiments agreed with the simulation results of Endo and Himeno [106].

Xu et al. [107] used the incompressible Navier-Stokes equations to model the fluid motion and the compliant surfaces were modeled as homogeneous spring-supported plates. They did not observe any DR in their simulation results. The differences in results obtained by Xu et al. [107] and Endo and Himeno [106] were due to the different averaging times used in their simulations.

Complexity in compliant surfaces is the reason that most of the past research done in this area is based on trial and error. Furthermore, Choi et al. [105] and Endo and Himeno [106] claimed that optimization and the right combination of material properties was necessary for compliant surfaces to achieve turbulent DR.

5. Microbubbles

Smaller bubbles with a diameter of 10 μm are known to be effective for DR [108], whereas larger bubbles with a diameter exceeding 500 μm tend to lose their DR efficiency [109]. These microbubbles can be produced in numerous ways, but the most common method is electrolysis. Microbubbles produced by electrolysis are forced through a porous medium as shown in Fig. 11.

The pioneers, McCormick and Bhattacharyya [112], created hydrogen microbubbles through water electrolysis on a ship hull's prototype, which reduced the viscous drag by 50% by altering the laminar and turbulent boundary layers. Microbubbles then gained much interest in the research field. Microbubbles could reduce the friction drag in the turbulent boundary layers by as much as 80% [113]. When the viscosity of microbubbles increased, the interaction between fluid and these bubbles was enhanced. As a result, Reynolds stress decreased, leading to reduction in near-wall velocity gradient, viscosity and density of the gas-liquid flow, hence drag was reduced [111].

Madavan et al. [114] performed numerical investigations on microbubbles DR over a flat plate using a simple mixing-length model for turbulence. DR up to 50% was obtained. The degree of DR was found to depend on the size and concentration of the bubbles, bubble dynamics, as well as the location of the injection and distributions of bubbles [114,115].

Most of the research on microbubbles has been done for external flow such as the flow over a flat plate, towed vehicle or ship [114, 116]. As for internal flow, the DR was attainable only for a limited distance after the injection point, as the bubbles coalesced and formed larger bubbles [109,117]. Afiza and Okanaga [109] observed that for the velocity range of 0.5-0.9 m/s, bubbles grew larger with time, and thus increased the friction loss in the pipe. They also concluded that bubble coalescence and size growth were affected by fluid velocity and pipe diameter. A trade-off between fluid velocity and pipe diameter might prevent bubble coalescence and size growth for optimal DR. Nevertheless, more investigations on a method to prevent bubble coalescence and size growth should be carried out. Furthermore, Xu et al. [117] did direct numerical simulation of turbulent channel flow using small spherical bubbles of average void fraction of 8%. Their findings were consistent with Kawamura et al. [108] that smaller bubbles produced sustained DR over time compared to larger bubbles. Larger bubbles only reduced drag for a short time before they increased drag. Kodama [118] studied the effect of microbubbles on skin friction reduction in pipe flow, and reported DR up to 40%. Wu et al. [119] managed to get 21.6% microbubbles DR in a channel flow.

6. Fiber

Forrest and Grierson [120] were the first to study the reduction of energy loss in a turbulent pipe flow using wood-pulp fiber-water suspensions. Asbestos, nylon, acrylic and glass fibers were also reported to suppress turbulence in suspensions. Asbestos fibers are hair-like and long, while nylons are generally of aspect ratio (length to diameter ratio) of 50 [6].

Fibers varied the velocity profile of the flow, thus then reducing the wall shear stress and lowering the flow resistance [121]. On the other hand, Lee and Duffy [122] discovered that the near-wall flow behavior was unaffected by the presence of fibers, and they proposed that the DR by fibers was due to the turbulence suppression in the turbulent core region.

Fibers with an aspect ratio of 25-35 were found to be effective at high concentration [6,123,124]. DR generally increased with the increasing fiber concentration. It was reported that 100 ppm of asbes-

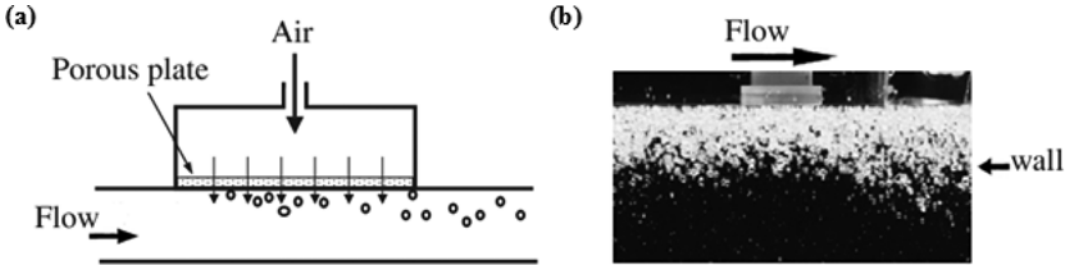

Fig. 11. (a) Schematic of a microbubbles generator [110], (b) microbubbles generated [111].

tos could reduce drag by 2%; while by increasing the concentration to 5,000 ppm, a DR of 70% could be achieved. Moreover, fibers with a higher aspect ratio, flexibility and surface roughness produced better DR. For two fibers with the same aspect ratio, the one with smaller diameter gave more DR, as flexibility increased with short diameter fibers [125]. Generally, it can be concluded that fibers with shorter diameter, higher aspect ratio and concentration, produce better DR.

Moyls and Sabersky [126] obtained a friction reduction by a factor of 3 for 300 ppm asbestos in a smooth pipe. Paschkewitz et al. [127] numerically studied turbulent DR using rigid fibers and reported a DR of up to 26%. When drag was reduced, Reynolds stresses, velocity fluctuation in the wall-normal and spanwise directions, and streamwise vorticity were also reduced, whereas streamwise fluctuations were increased. The results also showed that the elastic property was not essential for turbulent DR.

7. Surfactants (Surface Active Agents)

DR using an anionic surfactant, aluminium disoap was first discovered by Mysels [128] in 1949. Surfactants can be classified into two main classes of nonionic (undissociated) and ionic surfactants. Ionic surfactant can be further grouped into anionic (negative charge), cationic (positive charge) and zwitterionic (both positive and negative charges) surfactants. Surfactants align themselves into assemblies known as micelles, due to their polarity if the critical micelle concentration is reached [129].

Tamano et al. [130] studied the drag reducing ability of AROMOX, a nonionic surfactant, and found that with 500 ppm of it, DR ratio of 50%, and larger than 60% could be achieved in the turbulent boundary layer flow and pipe flow, respectively. It was also reported that the turbulence was suppressed and near-wall vortices were modified by the addition of AROMOX. For anionic surfactant like aluminium dioleate, a higher concentration of 7,500 ppm was required for DR to occur compared to other types of surfactants [131]. Moreover, a cationic surfactant, hexadecyltrimethyl ammonium chloride with sodium salicylate could reduce the drag of a rough pipe flow up to 73.7% [132]. As for zwitterionic surfactants, Wei et al. [133] found that a mere 200 ppm of oleyl trimethyl aminimide could reduce drag up to 83%.

Krope and Lipus [134] developed a mathematical model for the optimization of pipeline and pumps in heating and cooling systems with surfactants, and reported 80% DR. Yu and Kawaguchi [135] in their direct numerical simulation of surfactants in a channel, reported a maximum DR of 53.2%.

Yu et al. [136] performed experiments and direct numerical simulation with the Giesekus model for cetyltrimethyl ammonium chloride (CTAC) surfactant solution in a channel. They observed a dual effect of surfactants on frictional drag. Surfactants introduced a viscoelastic shear stress that increased the frictional drag, while at the same time, surfactants also dampened the turbulent eddies, decreased the turbulent shear stress, and thus decreased the frictional drag. The latter effect was larger than the former, so overall, it led to DR.

DR was caused by the shear-induced structures (SIS) of the surfactant solution [137-139]. Hu and Matthys [138] looked into the SIS structure of tris (2 hydroxyethyl) tallowalkyl ammonium acetate (TTAA) surfactant solution. The results indicated that the SIS recovered after shear. It took a longer time for the SIS to reform when a higher shear rate was applied to the surfactant solution.

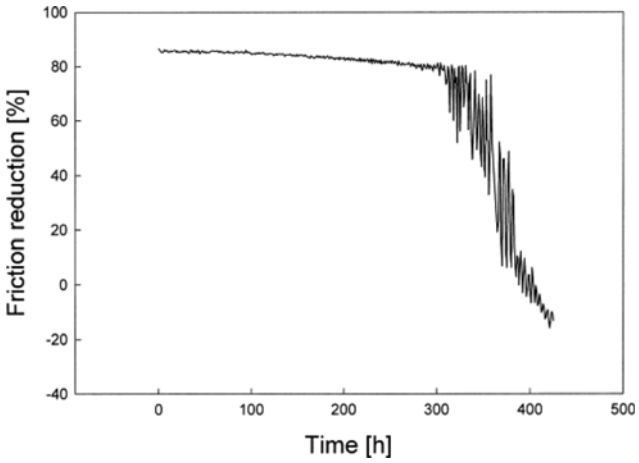

Fig. 12. Experimental results obtained by Kim et al. [139] from a pilot scale equipment for 200 ppm of Habon-G surfactant solution.

Zhang et al. [140] examined the DR characteristic of the CTAC surfactant solution in a turbulent channel flow, and compared its rheological characteristic with macroscopic behavior, to get an insight into the DR mechanism. For higher surfactant concentration, they observed a sudden increase in surfactant shear viscosity, after the initial decrease when the critical shear rate was reached. This showed the existence of SIS. However, these types of results were not obtained for concentrations lower than 90 ppm. They concluded that SIS was not necessary for surfactant DR. This conclusion was contradictory to those from Bewersdorff and Ohlendorf [137], Hu and Matthys [138] and Kim et al. [139].

Kim et al. [139] experimentally investigated the time dependent DR ability of the Habon-G surfactant solution. When the surfactant solution was subjected to a highly turbulent flow, there was a great reduction in its DR ability after a period of time as in Fig. 12. They termed this phenomenon as 'break down'. SIS for DR could not be formed in the broken-down solution. As illustrated in Fig. 13, before the breakdown, the surfactant solution was homogeneous but with some transparent undissolved parts. Large particles were identified after the breakdown and more of these particles were observed after more shearing was applied to the solution. These particles were believed to be aggregates of surfactant molecules. It was postulated that the phenomenon of breakdown was caused by the loss of effective micelle concentration, due to the precipitation of surfactants and the reaction with molecules of dissolved oxygen.

Degradation of surfactant was also discovered by Qi et al. [141]. They checked the DR ability of zwitterionic/anionic surfactant solution after subjecting it to 60 hours of mechanical shear. Although surfactant has self-repair ability after shear, it was found that the surfactant solution lost it DR efficiency completely at 70. °C Significant loss of DR capability was also observed for the combination of lower temperature, and high Reynolds number range.

8. Comparison between Drag Reducing Methods

DR through additives is the widely preferred method owing to its simplicity. No installation and maintenance costs are involved

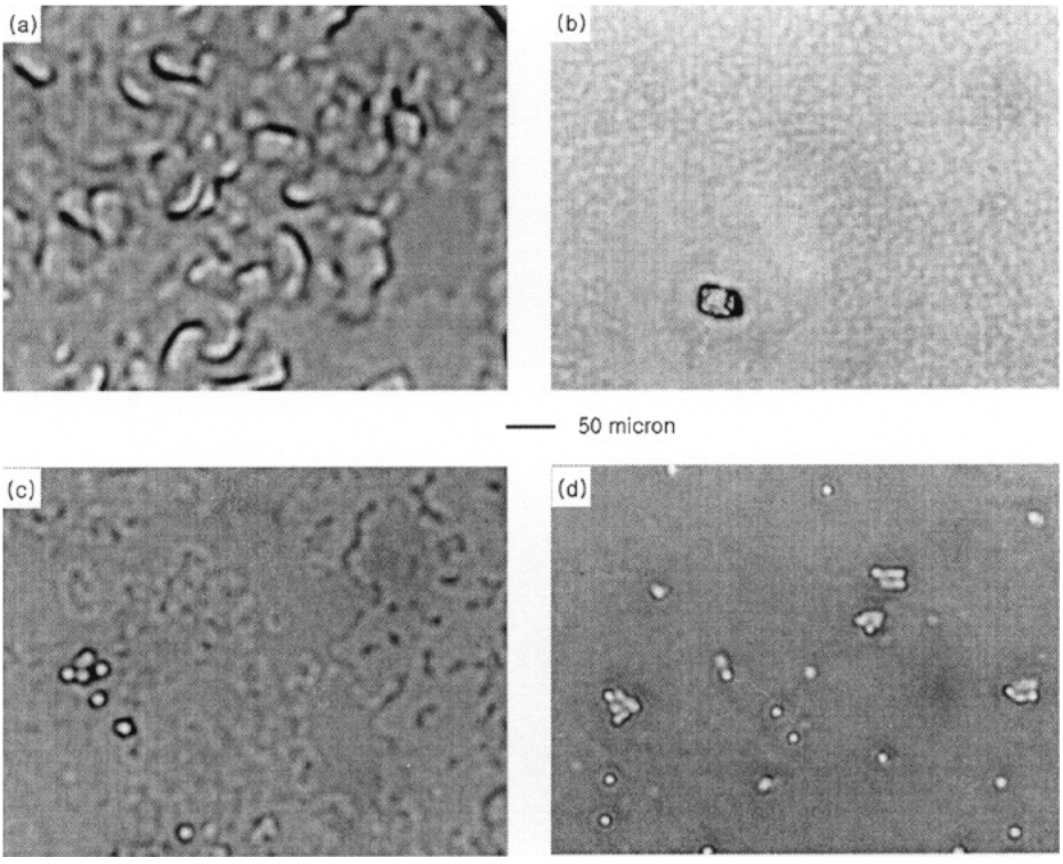

Fig. 13. Microphotographs of Habon-G surfactant solution [139]: (a) 1,000 ppm of fresh Habon-G solution, (b) before break down, (c) just after break down, (d) broken-down solution after more shearing.

as there are for riblets, dimples, oscillating walls, compliant surfaces and microbubbles. However, the non-additive DR methods are environmentally friendly, while drag reducing additives are toxic and environmental pollutants. In addition, DR through additives is not suitable for industries such as pharmaceutical and food processing, where fluid properties and parameters are essential for product quality. To apply drag reducing additives in these industries, additional stages are required. These additional stages might be costly and hence nullify the cost savings of additives. Although polymer additives might not be suitable for some industries, there is still a wide range of possible applications, especially in gas-liquid and liquid-liquid flow systems. Polymer additives have been proposed for applications such as oil field operations, slurry or hydraulic capsule pipeline transportation, suppression of atherosclerosis, prevention of lethality from hemorrhagic shock, increased water flow and water jet focusing in fire-fighting equipment, prevention of overflow in sewage systems, hydropower and irrigation systems, and as anti-misting agent in jet fuel [129].

In terms of DR performance, all the DR methods are found to reduce drag to some extent. Cheng et al. [142] recommended polymer additives as the most effective way of DR, even though other DR methods have been proven to work as well. To achieve similar turbulent DR as polymer additives, higher concentrations of fibers, ionic and nonionic surfactants are required, where the polymer can offer drag decrement of 80% just by a few parts per million (ppm) of it. Nevertheless, the serious drawback of polymer additives is that they tend to degrade and lose their effectiveness under high shear (increases with the increasing Reynolds number) and temperature. Mechanical degradation of polymer is mostly encountered for flow in a very long channel, or closed loop, with multiphase cycle through pumps. Surfactants, too, degrade under shear. However, surfactants have rapid self-regenerating ability after shear. Although surfactants have self-repair ability, they can completely lose their DR efficiency under extreme shear conditions. Moreover, surfactants cause precipitation and foaming. They are also sensitive to ions present in water.

Among the non-additive DR methods, riblets are the most studied. However, the maximum achievable DR practically is merely 8%; this is far lower than what polymers can offer. The DR performance of polymer additives can be 4-8 times more than riblets. Although a great deal of research has been done on riblets, it is still difficult to produce a riblet configuration that can push the DR performance past 10%. Dimples are mainly investigated for heat transfer enhancement. The suitability of dimples for DR is still uncertain, as mixed results have been reported by researchers. As for compliant surfaces, it involves complex issues in modeling and making them, thus more work needs to be done before they can be implemented for good DR performance. Oscillating walls can be an option for DR, but the process involved for installation and maintenance is complex. Microbubbles can reduce drag more than other non-

Table 2. Table of comparison between different drag reducing methods

DR methods	Advantages	Disadvantages
Riblets	• Maximum achievable DR reported is up to 10%. • Easy to be used [61]. • Require little or even no maintenance process [61]. • Environmental friendly.	• Theoretical DR by riblets is in the order of 10%, but riblets can only achieve 5-8% DR practically [70]. • Cost for restructuring pipe or duct to fix in riblets is expensive. • Inaccurate riblets configuration can lead to drag increment. It is complex to create a riblet configuration that produces satisfactory DR performance [61]. • There is no general agreement on the DR mechanisms of riblets. • Factors affecting the riblets DR such as riblets spacing are poorly understood [61].
Dimples	• Capable to reduce drag by 35% is reported in literature. • Environmental friendly.	• Most work done for dimples is for heat transfer enhancement studies and not on DR. • Result on DR was not consistent as the geometry of dimples studied, fluid initial condition, result measurement and analysis method are different. • DR achievable by dimples is small and even negligible. It is debatable in literature whether dimples are suitable to be used for DR.
Oscillating walls	• Maximum achievable DR reported is up to 46%. • Net energy saving by 7.3-10%. • Environmental friendly.	• Installation and maintenance processes are complex [61].
Compliant surfaces	• Maximum achievable DR reported is up to 60%. • Environmental friendly.	• Capable to reduce drag by 60% reported by Kramer cannot be reproduced by other researchers. • It is complex to simulate compliant surfaces.
Microbubbles	• Maximum achievable DR reported is up to 80%. • Low cost. • Environmental friendly.	• Microbubbles are more suitable practically for DR involving ocean vehicles like ships compared to fluid flow in pipes [116]. • For pipe flow, bubbles tend to coalesce and DR will diminish. In worst case, drag might increase due to larger bubbles size. • Mechanisms of microbubbles DR and quantification of its effect on DR are complex and inadequately understood [109,119].
Fibers	• Subjected to less shear degradation and more resistant to high stress compared to polymer additives [5,143]. • Less sensitive to temperature and viscosity variation of the solvent compared to polymer [5]. • Chemically and mechanically stable [123]. • Effective at broader temperature range [123].	• Induce plugging problems due to requirement of high concentration for efficient DR [123]. • Might alter the physical and chemical properties of the solvent which make them unsuitable to be used in industries which fluid parameters are important [61].

Table 2. Continued

DR methods	Advantages	Disadvantages
Surfactants	• Maximum achievable DR reported is up to 80% [33]. • Have self-assembling ability after shear, so the micelles recover and self regenerate rapidly after shear if the shear stress is lower than the critical shear stress [61,129,141]. • Widely applied in heating and cooling system [33, 129,134,144]	• Less attention is given to surfactant drag reducers and they are mainly being used only for gas-liquid flow system [145,146]. • Might alter the physical and chemical properties of the solvent which make them unsuitable to be used in industries which fluid parameters are important [61]. • Will still lose their DR ability if a critical value of Reynolds number and shear stress is exceeded [141,147]. • Might be toxic and hazardous to the environment [148].
	Nonionic surfactants	
	• Chemically stable [33]. • Low toxicity [33]. • Biodegradable [33].	• Do not carry any charge and thus cannot have reaction with other ions to form micelles, leading to their restricted applications [129]. • Only effective as drag reducers at narrow temperature range and concentration [144, 149-152].
	Cationic surfactants	
	• Effective drag reducer. • Recover rapidly from shear [144]. • Have wider effective temperature range [144]. • Encounter fewer problems like foam [144]. • Not sensitive to ions present in water like calcium and magnesium ions [33].	• Not easily biodegradable.
	Anionic surfactants	
	• Known as the only effective drag reducing additives for hydrocarbon transportation systems [129,153]. • Mechanically stable [154].	• High concentration is required for better DR performance, resulting in larger costs and environmental impacts [131]. • Vulnerable to ions present in tap or sea water like calcium and magnesium ions [155]. • Cause precipitation and foam [155].
	Zwitterionic surfactants	
	• Have wider effective temperature range [33].	• Sensitive to ions present in water as they have both positive and negative charges [33].
Polymers	• Capable to reduce drag up to 80% by low concentration. • Most studied DR additives [5]. • Have been widely applied as drag reducers in gas-liquid and liquid-liquid flow systems [156-163].	• Subjected to mechanical degradation as their bonds rupture and their ability to reduce drag diminishes at high pumping shear rate especially for closed-loop systems. • Subjected to thermal degradation especially at high temperature. • Might alter the physical and chemical properties of the solvent which make them unsuitable to be used in industries which fluid parameters are important [61]. • Might be toxic and hazardous to the environment [15,61].

additive DR methods, as shown in Table 2. The maximum reported DR for microbubbles is 80%, which is comparable with polymer additives, but the mechanism for DR and quantification of its effect on DR are complex and inadequately understood. In addition, in pipe flow, bubbles tend to coalesce, causing the DR to diminish. Also, drag tends to increase due to larger bubbles size.

Polymer additives are good because of their excellent DR efficiency, although they degrade over time. Mechanical degradation is not a good reason to stop using polymer additives for DR. Moreover, more investigations have been done on polymer additives as compared to other DR methods. Therefore, study on polymers is still a very attractive research field.

LAMINAR HEAT TRANSER ENHANCEMENT BY POLYMER ADDITIVES

1. Experimental Works Related to Laminar Heat Transfer Enhancement of Polymer Additives

Polymer additives behave differently in laminar flow as compared to turbulent flow. Polymer additives are found to enhance heat transfer without penalty of increased drag in the fully developed laminar non-circular flow. Oliver and Karim [8] studied laminar flow heat transfer in flattened tubes using a PAA solution. Flattened tubes gave higher heat transfer coefficient than a circular tube. This increment was believed to be caused partly by the increment in the tube-wall shear rate, and partly by the effect of induced secondary flow. Heat transfer coefficient could be increased by over 90%, due to the increment in the tube-wall shear rate. Without considering the effect of increment in the tube-wall shear rate, the heat transfer could be increased by 45%, due to the sole effect of the induced secondary flow. Moreover, higher tube-wall shear rate was found in tubes with higher aspect ratio, which in turn contributed to a higher heat transfer coefficient, but at the expense of a larger drop in pressure. Secondary flow effect became negligible at higher aspect ratio (5.7), but reached a maximum with the aspect ratio of 1.5. The optimum aspect ratio for good heat transfer performance, with small penalty in pressure drop, was found to be 1.4.

Mena et al. [9] compared the laminar flow heat transfer of viscoelastic solution in various pipes, with different cross sections under constant wall temperature boundary condition. They observed that for a pipe with rectangular cross section, polymer additives enhanced the heat transfer coefficient of up to 50% when compared to a circular pipe (Fig. 14). This was due to the development of secondary flow, resulting from normal stress difference. Square and triangular ducts showed less heat transfer improvement compared to the rectangular pipes. It was examined that secondary flow had little effect on flow rate for all non-circular ducts studied. Besides, no effect on fluid friction was reported. The presence of secondary flow in laminar non-circular ducts was observed by several researchers [164-167]. Gao [168] remarked that the heat transfer enhancement increased with the increasing strength of secondary flow.

Hartnett and Kostic [10] studied heat transfer characteristics using PAA additives in water for a 2 : 1 rectangular channel. The local and mean Nusselt numbers were found to be higher, and thus a larger heat transfer rate than using pure water at the same Rayleigh

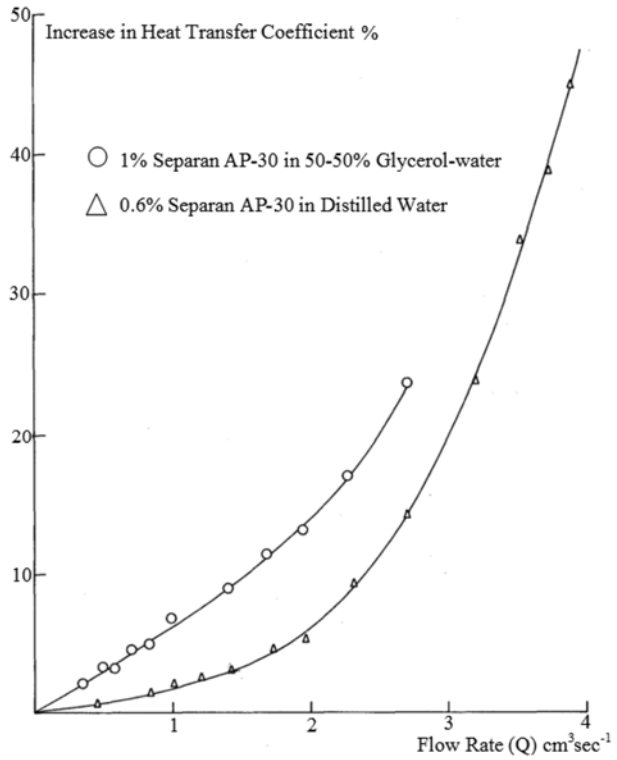

Fig. 14. Increase in heat transfer coefficient versus flow rate for a rectangular duct when compared to a circular pipe [9].

number. Hartnett and Kostic [10] agreed with Mena et al. [9] that the heat transfer enhancement was due to the secondary flow. In addition, the measured pressure drop agreed with the prediction based on the power law model. Since no flow visualization results had been obtained, Hartnett and Kostic [10] concluded that viscoelastic PAA behaved like a purely viscous non-Newtonian fluid in laminar non-circular flow, and was similar to the case of laminar circular flow. The elasticity of PAA did not have an appreciable influence on pressure drop; thus the friction factor behavior remained undisturbed. Kostic [6] hypothesized that the reason for no increment in the friction might be due to the secondary flow, which was in the transverse direction.

Xie and Hartnett [169] conducted experiments using carbopol 934 (polyacrylic acid) and PAA (separan AP-273) in a 2 : 1 rectangular duct. Under top-wall-heated thermal boundary condition, the local Nusselt number of both the polymeric solutions was measured to be two to three times higher than water. The friction factor result is shown in Fig. 15 and it is in good agreement with that obtained by Hartnett and Kostic [10]. In addition, polymers with higher elasticity were found to produce higher heat transfer enhancement.

Rao [170,171] studied the heat transfer behavior of PAA and hydroxyethyl cellulose in a 5 : 1 rectangular duct. When compared to the 2 : 1 rectangular duct used by Hartnett and Kostic [10], Rao's experimental data showed that there was only a slight increase in the heat transfer of the solutions as compared to water. The heat transfer performance in the 2 : 1 rectangular duct was better than in the 5 : 1 rectangular duct. It was suggested that 5 : 1 rectangular

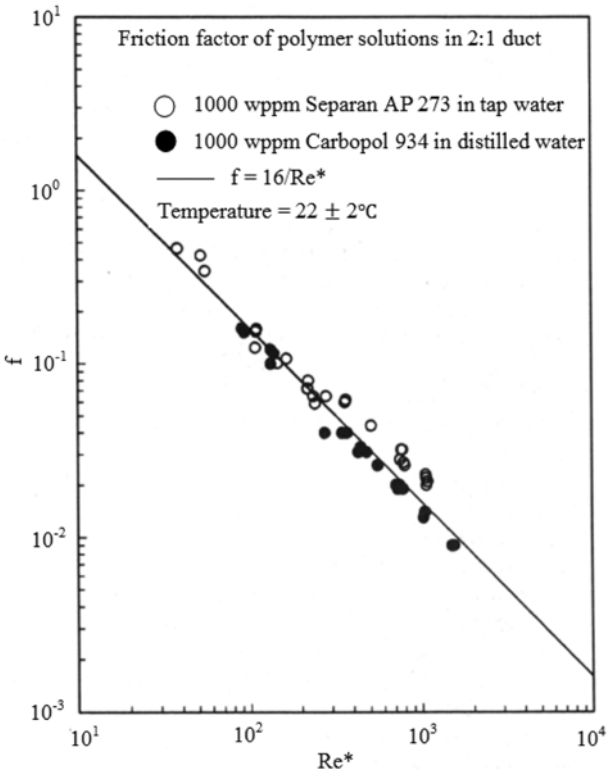

Fig. 15. Friction factor of 1,000 ppm aqueous PAA and Carbopol solution in a 2 : 1 rectangular duct [169].

duct produced weaker secondary flow, and thus a smaller increment in the heat transfer performance. The effect of secondary flow was more significant for the 2 : 1 rectangular duct. On the other hand, the laminar fanning friction factor obtained agreed with the Newtonian correlation for isothermal values for all the concentration range tested.

Hartnett and Kostic [39] also reported that for a square duct with boundary condition of heated top wall, the laminar heat transfer could be increased up to 200-300% as compared to Newtonian fluid, when aqueous polymer or carbopol solutions were used. The heat transfer enhancement was caused by the same secondary flow, which improved the heat transfer in rectangular ducts. The secondary flow did not affect the pressure drop for the square duct to the same degree.

In contrast to laminar non-circular flow, polymer additives do not help in heat transfer augmentation in laminar circular flow. In 1982, Cho and Hartnett [17] measured the fully established pressure losses and heat transfer for laminar flow in circular tube and concluded that elasticity played no vital role on the friction factor and heat transfer in a fully developed laminar circular flow. Their results revealed that the experimental values of heat transfer and pressure losses conformed well to the predicted values using the power law model developed for non-Newtonian fluids. Hartnett [16] claimed that for a steady state laminar flow through a circular pipe, the polymeric solution behaved the same as a purely viscous fluid, as there was no mechanism showing the elastic nature of the polymer additives. Only under unsteady flow, such as pulsating flow and entrance region flow, was the elasticity of polymer additives manifested.

2. CFD Studies Related to Laminar Heat Transfer Enhancement of Polymer Additives

Shin and Cho [38] investigated the effects of temperature-dependent and shear thinning viscosity of non-Newtonian PAA flow on laminar heat transfer in a 2 : 1 rectangular duct under constant axial heat flux, and constant peripheral wall temperature condition. The effect of secondary flow on the heat transfer was excluded in their study. A parabolic velocity profile, no slip condition along duct periphery for axial velocity component, and assumption of an axially-parallel flow were defined for the simulation. Solutions were obtained numerically via finite volume methods, and the local Nusselt number was found to be in good agreement with the experimental results of Xie and Hartnett [169]. Under the effect of temperature dependent and shear thinning viscosity of the PAA solution, the Nusselt number was enhanced by 70-300% as compared to the constant fluid property. The heat transfer enhancement was attributed to the increasing near-wall velocity gradient due to the combined effects of temperature dependent and shear thinning viscosity.

Naccache and Mendes [59] examined the heat transfer performance of a polymeric solution in a rectangular duct for laminar regime. The viscoelastic property of the polymeric solution was represented using Criminale-Ericksen-Filbey (CEF) constitutive equations. The boundary conditions employed were no slip for velocity at walls, symmetrically heated top and bottom walls, and adiabatic vertical side walls. They discovered that the heat transfer was enhanced, but the friction factor was basically unaffected by the secondary flow. The Nusselt number for this type of non-Newtonian solution was three times larger than the relative Newtonian flow due to the enhancement by secondary flow. For duct aspect ratio of 1, 2 and 4, the Nusselt number increment was 6-275%, 38-230% and 33-130%, correspondingly. In contrast to the results obtained by Shin and Cho [38], the effect of shear thinning viscosity on the heat transfer enhancement was negligible compared to the impact of secondary flow. This difference in result was due to the omission of the temperature effect by Naccache and Mendes [59].

POTENTIAL RESEARCH AREA: ADDITION OF DRAG REDUCING ADDITIVES TO NANOFLUID (DRAG REDUCING NANOFLUID)

Nanofluids have been attractive recently because of their promising potential to improve heat transfer efficiency of conventional heat transfer fluids. Nonetheless, the heat transfer enhancement by nanofluids is achieved at the expense of a higher pressure drop ascribed to the increment of fluid viscosity when nanoparticles are added to the heat transfer fluids [172-184]. An example of pressure drop increment for nanofluid system is reported by Samira et al. [184], as shown in Fig. 16. Samira et al. [184] concluded that the pressure drop of the nanofluid system increased with the increasing Reynolds number and nanoparticles concentration. Since the drag reducing additives are recognized for their DR capability, they might be a good option to improve the hydraulic efficiency of nanofluid, and mutually, the nanoparticles would help to improve the heat transfer performance of drag reducing fluids.

Recently, the addition of drag reducing agents into nanofluid

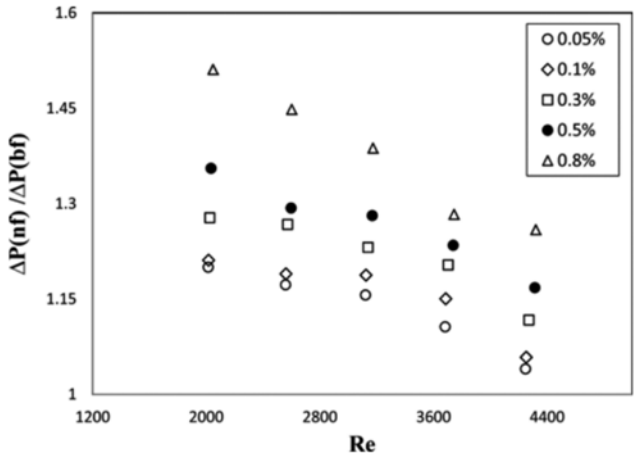

Fig. 16. The pressure drop ratio of the CuO nanofluid to the base fluid (a mixture of 60/40 ratio of ethylene glycol and distilled water), evaluated in the car radiator at 35 °C inlet temperature [184].

has been reported for turbulent circular flow. Liu and Liao [185] studied the forced convective heat transfer performance of drag reducing fluid with the addition of nanoparticles. They used carbon nanotubes and water doped with CTAC surfactant drag reducing fluid in a 25.6 mm diameter circular tube. In their experiments, the DR ability of the CTAC solution was maintained, even with the addition of carbon nanotubes, as shown in Fig. 17(a). However, to approach a similar DR effect of the conventional CTAC solution, more CTAC was required. Some of the CTAC molecules attached to carbon nanotubes, which in turn reduced the availability of CTAC molecules to form rod-shaped micelles for DR. Furthermore, the heat transfer performance of the CTAC solution was significantly improved by the addition of carbon nanotubes (Fig. 17(b)). The heat transfer performance of CTAC-nanofluid system was found to depend on the fluid temperature, nanoparticle concentration, and surfactant concentration.

Drzazga et al. [186] investigated experimentally the effect of nonionic surfactants in metal oxide-water nanofluid on DR in a 4 mm diameter pipe, with Reynolds number between 8000 to 50000. The nonionic surfactants used were Rokacet O7 and Rokanol K7, while the metal oxide nanofluid was copper (II) oxide. They did not carry out any studies on the effect of nonionic surfactants on nanofluid heat transfer. Their results showed that nonionic surfactants in nanofluid still had the ability to reduce drag, while the nanoparticles had a negligble impact on the DR. Better DR performance was reported for higher surfactant concentration, but the viscosity of the solution increased with the increase of surfactant concentration. A significant increment in the solution viscosity might hinder the DR phenomenon. Therefore, the trade-off between the DR performance and viscosity increment was essential to obtain optimal surfactant concentration for the best DR performance.

There were also experimental investigations on the thermal conductivity and shear viscosity of viscoelastic-fluid-based nanoparticles (VFBN), which was the addition of nanoparticles in viscoelastic CTAC/Sodium salicylate solution [187,188]. It was found that the suspension of nanoparticles in the VFBN increased the thermal conductivity of the base fluid, showing its potential ability to enhance convective heat transfer. In addition, VFBN exhibited a non-Newtonian shear thinning behavior, which is similar to the characteristic of the viscoelastic base fluid itself. Hence, it was suggested that VFBN might also have the turbulence drag reducing ability.

Yang et al. [189] performed experiments on heat transfer and flow resistance using viscoelastic-fluid-based Copper (Cu) nanofluid. The viscoelastic-based-fluid (VBF) used was CTAC/Sodium Salicylate (NaSaI) with mass concentration of 600 and 1,200 ppm. The tested volume fraction range of Cu nanoparticles was 0.25, 0.5 and 1.0 vol%. It was observed that the VFBN showed improved heat transfer characteristics compared to the VBF (Fig. 18). This enhancement was attributed to the enhanced thermal conductivity, and it increased with the increaing Cu nanoparticles volume fraction. The VBF did not lose its DR ability when suspensions of nanoparticles were added to it; however, the drag reducing effect was weakened, as presented in Fig. 19. Furthermore, when the temperature was increased, the heat transfer coefficient of the VFBN increased, while there was not much influence of temperature on pressure drop. They concluded that the VFBN showed both the

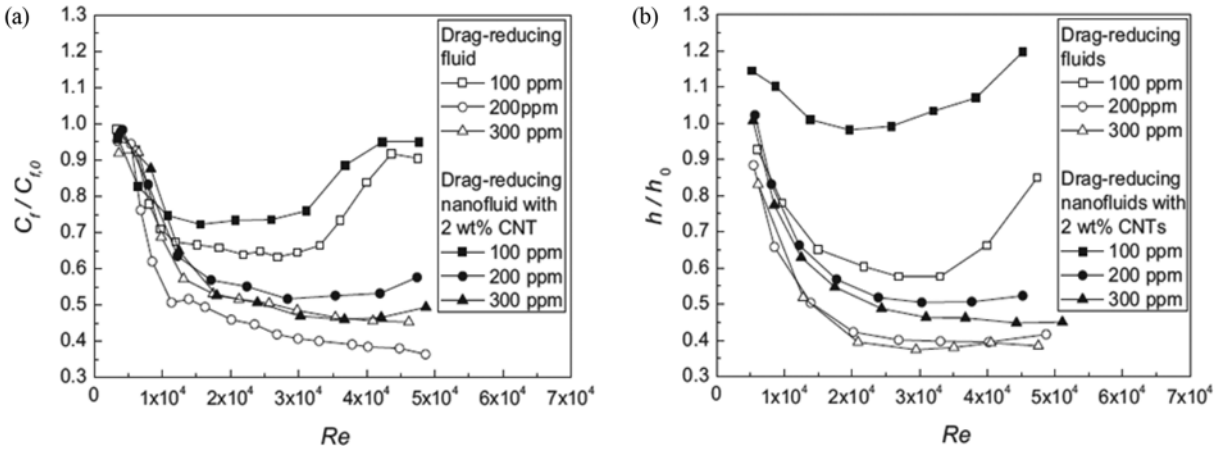

Fig. 17. (a) Fanning factor ratio of drag reducing CTAC-nanofluid to water at 22 °C, (b) heat transfer coefficient ratio of drag reducing CTAC-nanofluid to water at 22 °C [185].

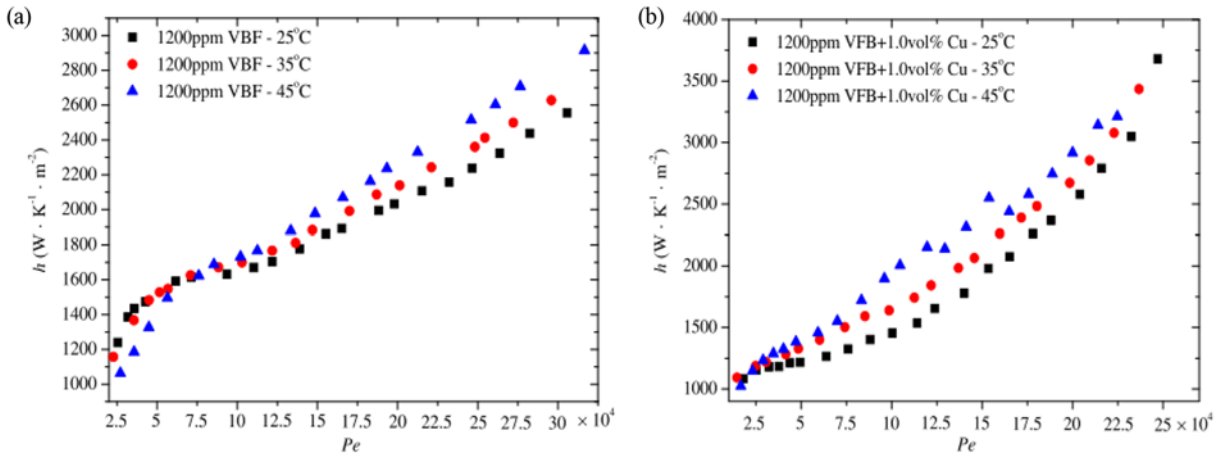

Fig. 18. Influence of temperature on convective heat transfer coefficient: (a) 1,200 ppm VBF flow cases, (b) VBFN flow cases [189].

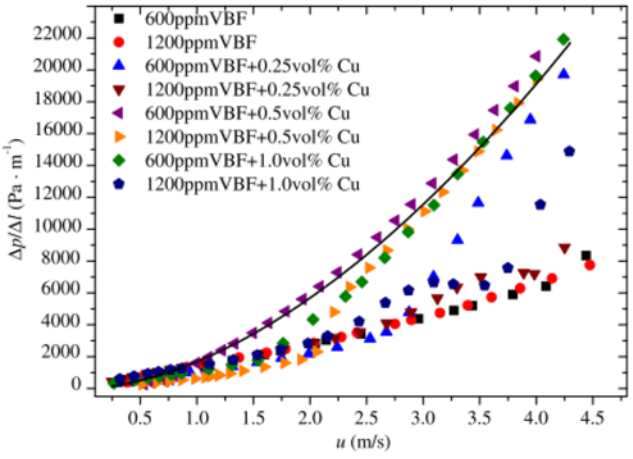

Fig. 19. Variation of pressure drop per unit length with velocity for VFBN with different nanoparticles concentration, and different VBF concentration [189].

features of VBF and nanofluid. The synergetic effect of viscoelasticity and nanofluid characteristics were dependent on the rheological and physical properties of the base fluid, as well as the flow condition (velocity).

Kostic [190,191] suggested the development of a new hybrid drag reducing fluid (POLY-nanofluid). He postulated that the nanoparticles might yield heat transfer augmentation, while the polymer might enhance the flow properties, such as a reduced flow friction and pressure drop. The long-chain polymers are believed to have active chemical and physical interactions with the nanoparticles, which in turn open many more unprecedented applications in the future, but more investigations are needed. A thermal conductivity measuring apparatus for this poly-nanofluid has been developed by Walleck [191,192].

KNOWLEDGE GAP AND FUTURE RESEARCH DIRECTIONS

Over the past decades, much work has been devoted to investigate the DR by polymer additives, its mechanisms, factors affecting DR performance, applications of drag reducing polymers, and its heat transfer behavior. However, research to study the effect of drag reducing agents in nanofluid is scarce. To date, no research has been reported on both experimental and CFD modeling of the use of drag reducing agents-nanofluid system in non-circular ducts covering laminar and turbulent regimes. In addition, no experimental work and CFD modeling has been carried out for drag reducing agents-nanofluid system in circular laminar flow. CFD modeling on turbulent flow of drag reducing agents-nanofluid system in circular pipe has not been researched as well. Recent studies on drag reducing agents-nanofluid system are based on the addition of surfactants in the nanofluid; less attention has been given to the addition of polymer additives to nanofluid. Therefore, it is novel to study the effect of polymer additives on nanofluid. Although the DR in laminar flow is not practical theoretically, the addition of drag reducing polymer might help to improve the hydraulic efficiency of the fluid flow; thus, it is also important to study the effect of polymer additives on nanofluid in laminar flow for both circular and non-circular ducts.

Polymer-nanofluid system can be termed as POLY-nanofluid. The addition of polymer additives into nanofluid might help to improve the current limitations of nanofluid system, particularly at a high volume fraction of nanoparticles. On the other hand, polymer additives might impose an adverse effect on the nanofluid. Therefore, it is also recommended to study the fluid flow behavior and the heat transfer performance of POLY-nanofluid, via integrated experiments and simulation work. Both experiments and simulations should cover both laminar and turbulent regimes.

The rheological behavior of POLY-nanofluid might be different from pure polymer and nanofluid solutions. Viscosity is an important property in thermal applications that employ fluid flow, because it measures the internal resistance of fluid flow and is related to the required pumping power of the system [193-197]. As a result, an understanding of the rheological behavior of POLY-nanofluid may be a future research direction. Furthermore, the study of degradation is also important for POLY-nanofluid to assess its feasibility and applicability in industrial applications.

Nanofluid can be modeled using single phase, two-phase dispersion and mixture models in CFD. Since, as mentioned earlier,

Table 3. Targets for potential future research

Future research directions	Targets
POLY-nanofluid	• Understand the effect of polymer on the rheology, heat transfer performance and fluid behavior of nanofluid for circular and non-circular ducts, covering both laminar and turbulent regimes. • Experimentally and numerically investigate the flow of POLY-nanofluid in circular duct. Experimental data will be used to validate the CFD model of POLY-nanofluid system in the circular duct. • Perform single-phase and two-phase modeling on the flow and heat transfer of POLY-nanofluid in non-circular duct using the validated CFD model. • Find the optimum concentration of polymer and nanoparticles in POLY-nanofluid system for maximum thermal-hydraulic efficiency. • Study how polymer degradation affects the performance of POLY-nanofluid system.

regarding the lack of proper constitutive equations to describe the polymer behavior, it is suggested that rheological study of polymer additives should be carried out. The rheological data can serve as an input to model the polymer behavior. Similar method can be applied in modeling the fluid behavior of POLY-nanofluid.

The experimental results obtained for POLY-nanofluid system in circular pipe can be used to validate the simulation results. The validated CFD results can then be employed to model the POLY-nanofluid in non-circular ducts. Additionally, it is suggested to obtain optimum concentrations of nanoparticles and polymer for better mechanical and thermal-hydraulic efficiency.

Targets for potential future research are summarized in Table 3. With these targeted research directions, contributions towards knowledge on POLY-nanofluid can be made, and lead to new insight into fluid rheology, flow behavior and heat transfer characteristics of POLY-nanofluid. Moreover, integrated experimental studies with simulations help to develop a reliable theoretical framework for POLY-nanofluid. These future directions will also aid in optimizingt the thermal-hydraulic efficiency of POLY-nanofluid so that the applications of polymers and nanofluid can be extended. Finally, the study of polymer degradation of POLY-nanofluid helps to give a better understanding of how it affects the performance of a system.

CONCLUSIONS

DR can be achieved through non-additive and additive methods. Non-additive DR methods include riblets, dimples, compliant surfaces, microbubbles and oscillating walls, while drag reducing additives comprise fibers, surfactants and polymers. Of all other methods, greater DR can be achieved by polymers with lower concentration. A value of 80% has been reported for polymer-induced DR. Although degradation is a serious issue of polymer application, it is attractive to do research with polymer owing to its high DR ability. Polymer additives can reduce drag in both closed and open turbulent flow. Besides research on turbulent DR, heat transfer performance of polymer additives is also studied in turbulent regimes. It was found that high polymer-induced DR is always accompanied by considerable heat transfer performance deterioration. Nonetheless, polymer additives enhance heat transfer in laminar non-circular flow without changing the fluid friction. Many researchers agree that this heat transfer augmentation is due to the secondary flow induced by polymer elasticity properties. Moreover, no heat transfer enhancement is recorded for polymer additives in laminar circular flow. Recently, there have been a few studies focusing on the effects of drag reducing additives on the flow behavior and heat transfer performance of nanofluid. Polymers might be a promising solution in addressing the limitations of nanofluid applications. Therefore, the POLY-nanofluid system is a potential and promising research field. Future research directions should focus on the fluid behavior and heat transfer characteristic of POLY-nanofluid. These potential research areas will help to improve and optimize the flow behavior and heat transfer performance of POLY-nanofluid. Moreover, the suggested research directions can aid to extend the applications of nanofluids and polymers.

ACKNOWLEDGEMENT

The authors gratefully acknowledge financial support from the Ministry of Higher Education (MOHE) Malaysia under Exploratory Research Grant Scheme (ERGS) ERGS/1/2012/TK05/CURTIN/02/1. The authors also thank anonymous reviewers for their valuable comments and feedback which significantly improve the quality of this manuscript.

NOMENCLATURE

C_f : fanning friction factor [-]
f : friction factor [-]
h : mean heat transfer coefficient [W/m^2 K]
Q : flow rate [cm^3/s]
vol% : volume percent [%]
$\Delta p/\Delta l$: pressure drop per unit length [Pa/m]
Pe : peclet number [-]
Pr : prandtl number [-]
Re : Reynolds number [-]
Re* : Kozicki generalized Reynolds number [-]
u : velocity [m/s]

Subscripts
o : base fluid (water)

REFERENCES

1. W. Brostow, *J. Ind. Eng. Chem.*, **14**, 409 (2008).
2. B. A. Toms, *Some observations on the flow of linear polymer solutions through straight tubes at large Reynolds numbers*, Proceedings

of the 1st International Congress on Rheology (1949).
3. E. D. Burger, W. R. Munk and H. A. Wahl, *J. Pet. Technol.*, **34**, 377 (1982).
4. G. C. Liaw, J. L. Zakin and G. K. Patterson, *AIChE J.*, **17**, 391 (1971).
5. P. Peyser, *J. Appl. Polym. Sci.*, **17**, 421 (1973).
6. M. Kostic, *Int. J. Heat Mass Trans.*, **37**, 133 (1994).
7. N. S. Berman, *Annu. Rev. Fluid Mech.*, **10**, 47 (1978).
8. D. R. Oliver and R. B. Karim, *Canadian J. Chem. Eng.*, **49**, 236 (1971).
9. B. Mena, G. Best, P. Bautista and T. Sanchez, *Rheol. Acta*, **17**, 454 (1978).
10. J. P. Hartnett and M. Kostic, *Int. J. Heat Mass Transfer*, **28**, 1147 (1985).
11. M. K. Gupta, A. B. Metzner and J. P. Hartnett, *Int. J. Heat Mass Transfer*, **10**, 1211 (1967).
12. P. S. Virk, E. W. Merrill, H. S. Mickley, K. A. Smith and E. L. Mollo-Christensen, *J. Fluid Mech.*, **30**, 305 (1967).
13. W. D. McComb and L. H. Rabie, *AIChE J.*, **28**, 547 (1982).
14. R. H. J. Sellin and M. Ollis, *Ind. Eng. Chem. Prod. Res. Dev.*, **22**, 445 (1983).
15. A. Abubakar, T. Al-Wahaibi, Y. Al-Wahaibi, A. R. Al-Hashmi and A. Al-Ajmi, *Chem. Eng. Res. Design*, **92**, 2153 (2014).
16. J. P. Hartnett, *J. Heat Transfer*, **114**, 296 (1992).
17. Y. I. Cho and J. P. Harnett, *Non-Newtonian fluids in circular pipe flow*, in *Advances in Heat Transfer*, J. P. Harnett and F. I. Thomas Eds., Elsevier, USA, 59 (1982).
18. E. Y. Kwack, J. P. Hartnett and Y. I. Cho, *Wärme - und Stoffübertragung*, **16**, 35 (1982).
19. E. Y. Kwack and J. P. Hartnett, *Int. Commun. Heat Mass Transfer*, **10**, 451 (1983).
20. N. J. Kim, S. Kim, S. H. Lim, K. Chen and W. Chun, *Int. Commun. Heat Mass Transfer*, **36**, 1014 (2009).
21. J. L. Lumley, *Annu. Rev. Fluid Mech.*, **1**, 367 (1969).
22. D. J. Fleming, *Capillary Rheometry*, Polymer Rheology' 99 Conference: Approach to Quality Control for the Plastics and Rubber Industries (1999).
23. C. D. Dimitropoulos, R. Sureshkumar and A. N. Beris, *J. Non-Newtonian Fluid Mech.*, **79**, 433 (1998).
24. D. Bonn, A. Yacine, W. Christian, D. Stéphane and C. Olivier, *J. Phys.: Condens. Matter*, **17**, S1195 (2005).
25. J. J. J. Gillissen, *Phys. Rev. E*, **78**, 046311 (2008).
26. J. M. J. D. Toonder, M. A. Hulsen, G. D. C. Kuiken and F. T. M. Nieuwstadt, *J. Fluid Mech.*, **337**, 193 (1997).
27. T. Min, J. Yul Yoo, H. Choi and D. D. Joseph, *J. Fluid Mech.*, **486**, 213 (2003).
28. T. T. Tung, K. S. Ng and J. P. Hartnett, *Lett. Heat and Mass Transfer*, **5**, 59 (1978).
29. P. S. Virk, H. S. Mickley and K. A. Smith, *J. Appl. Mech.*, **37**, 488 (1970).
30. M. Poreh and U. Paz, *Int. J. Heat Mass Transfer*, **11**, 805 (1968).
31. J. P. Hartnett and E. Y. Kwack, *Int. J. Thermophys.*, **7**, 53 (1986).
32. P. M. Debrule and R. H. Sabersky, *Int. J. Heat Mass Transfer*, **17**, 529 (1974).
33. R. P. Singh, *Drag reduction*, in *Encyclopedia of Polymer Science and Technology*, J. I. Kroschwitz Ed., John Wiley & Sons, Inc., New Jersey, 519 (2002).
34. R. H. J. Sellin, J. W. Hoyt and O. Scrivener, *J. Hydraulic Res.*, **20**, 29 (1982).
35. R. P. Singh, *Drag reduction*, in *Properties and Behavior of Polymers*, J. Bailey, A. Seidel, E. Arndt, S. Thomas, K. Parrish and D. Gonzalez Eds., John Wiley & Sons, Inc., New Jersey, 254 (2011).
36. K. H. Toh and A. J. Ghajar, *Int. J. Heat Mass Transfer*, **31**, 1261 (1988).
37. S. X. Gao and J. P. Hartnett, *Int. Commun. Heat Mass Transfer*, **19**, 673 (1992).
38. S. Shin and I. Y. Cho, *Int. J. Heat Mass Transfer*, **37** 19 (1994).
39. J. P. Hartnett and M. Kostic, *Heat transfer to Newtonian and non-Newtonian fluids in rectangular ducts*, in *Advances in Heat Transfer*, J. P. Hartnett and J. T. F. Irvine Eds., Academic Press, Inc., USA, 247 (1989).
40. W. K. Gingrich, Y. I. Cho and W. Shyy, *Int. J. Heat Mass Transfer*, **35**, 2823 (1992).
41. P. Escudier and S. Smith, *Proceedings of the Royal Society of London. Series A: Mathematical, Physical and Engineering Sciences*, **457**, 911 (2001).
42. M. Kostic and J. P. Hartnett, *Int. Commun. Heat Mass Transfer*, **12**, 483 (1985).
43. K. S. Yang, H. J. Choi, C. B. Kim, I. S. Kim and M. S. Jhon, *Korean J. Chem. Eng.*, **11**, 8 (1994).
44. C. A. Kim, D. S. Jo, H. J. Choi, C. B. Kim and M. S. Jhon, *Polym. Test.*, **20**, 43 (2001).
45. H. J. Choi, C. A. Kim and M. S. Jhon, *Polymer*, **40**, 4527 (1999).
46. C. A. Kim, J. T. Kim, K. Lee, H. J. Choi and M. S. Jhon, *Polymer*, **41**, 7611 (2000).
47. S. T. Lim, H. J. Choi, S. Y. Lee, J. S. So and C. K. Chan, *Macromolecules*, **36**, 5348 (2003).
48. S. T. Lim, H. J. Choi and C. K. Chan, *Macromol. Rapid Commun.*, **26**, 1237 (2005).
49. J. T. Kim, C. A. Kim, K. Zhang, C. H. Jang and H. J. Choi, *Colloids Surf., A: Physicochem. Eng. Asp.*, **391**, 125 (2011).
50. J. I. Sohn, C. A. Kim, H. J. Choi and M. S. Jhon, *Carbohydr. Polym.*, **45**, 61 (2001).
51. C. A. Kim, S. T. Lim, H. J. Choi, J. I. Sohn and M. S. Jhon, *J. Appl. Polym. Sci.*, **83**, 2938 (2002).
52. Z. Matras, T. Malcher and B. Gzyl-Malcher, *Thin Solid Films*, **516**, 8848 (2008).
53. A. A. Mohsenipour and R. Pal, *Canadian J. Chem. Eng.*, **91**, 190 (2013).
54. P. K. Ptasinski, B. J. Boersma, F. T. M. Nieuwstadt, M. A. Hulsen, B. H. A. A. Van Den Brule and J. C. R. Hunt, *J. Fluid Mech.*, **490**, 251 (2003).
55. V. E. Terrapon, *Lagrangian simulations of turbulent drag reduction by a dilute solution of polymers in a channel flow*, Ph.D. Thesis, Stanford University (2005).
56. M. T. Dhotre, K. Ekambara and J. B. Joshi, *J. Chem. Eng. Japan*, **40**, 304 (2007).
57. M. P. Escudier, F. Presti and S. Smith, *J. Non-Newtonian Fluid Mech.*, **81**, 197 (1998).
58. F. Presti, *Investigation of transitional and turbulent pipe flow of non-Newtonian fluids*, Ph.D. Thesis, University of Liverpool, UK (2000).
59. M. F. Naccache and P. R. S. Mendes, *Int. J. Heat Fluid Flow*, **17**, 613 (1996).
60. B. Dean and B. Bhushan, *Philosophical Transactions of the Royal*

Society A: Mathematical, Phys. Eng. Sci., **368**, 4775 (2010).
61. H. A. Abdulbari, R. M. Yunus, N. H. Abdurahman and A. Charles, *J. Ind. Eng. Chem.*, **19**, 27 (2013).
62. R. García-Mayoral and J. Jiménez, *Philos. Trans. R. Soc. A: Mathematical, Phys. Eng. Sci.*, **369**, 1412 (2011).
63. J. B. Huang and C. M. Ho, *Microriblets for drag reduction*, Smart Structures and Materials 1995: Smart Electronics (1995).
64. M. J. Walsh, *Drag characteristics of v-groove and transverse curvature riblets*, in *Viscous Flow Drag Reduction*, G. R. Hough Ed., American Institute of Aeronautics and Astronautics, Washington, 168 (1980).
65. M. J. Walsh, *Riblets*, in *Viscous Drag Reduction in Boundary Layers*, D. M. Bushnell and J. N. Hefner Eds., American Institute of Aeronautics and Astronautics, Washington, 203 (1990).
66. C. K. Liu, S. Klein and J. Johnston, *An experimental study of turbulent boundary layer on rough walls*, Stanford University, Department of Mechanical Engineering (1966).
67. H. Choi, P. Moin and J. Kim, *Phys. Fluids A: Fluid Dynamics*, **3**, 1892 (1991).
68. D. C. Chu and G. E. Karniadakis, *J. Fluid Mech.*, **250**, 1 (1993).
69. K. S. Choi, *J. Fluid Mech.*, **208**, 417 (1989).
70. C. Warsop, *Turbulent drag reduction methods - Current status and prospects for turbulent flow control*, in *Aerodynamic Drag Reduction Technologies: Proceedings of the CEAS/DragNet European Drag Reduction Conference*, P. Thiede Ed., Springer, Germany, 269 (2001).
71. H. Choi, P. Moin and J. Kim, *J. Fluid Mech.*, **255**, 503 (1993).
72. A. Baron, M. Quadrio and L. Vigevano, *Int. J. Heat Fluid Flow*, **14**, 324 (1993).
73. E. Bacher and C. Smith, *A combined visualization-anemometry study of the turbulent drag reducing mechanisms of triangular microgroove surface modifications*, American Institute of Aeronautics and Astronautics, Shear Flow Control Conference (1985).
74. V. V. Alekseev, I. A. Gachechiladze, G. I. Kiknadze and V. G. Oleinikov, *Tornado-like energy transer on three-dimensional concavities of reliefs-structure of self-organizing flow, their visualization, and surface streamlining mechanicms*, in *Transactions of the 2nd Russian Nat. Conf. of Heat Transfer, vol. 6, Heat Transfer Intensification Radiation and Complex Heat Transfer*, Publishing House of Moscow Energy Institute (MEI), Moscow, 33 (1998).
75. S. Aoyama, Golf ball dimple pattern, US Patent, 5,957,786 (1999).
76. A. Kasashima, Golf ball, US Patent, 6,761,647 (2004).
77. L. L. M. Veldhuis and E. Vervoort, *Drag effect of a dented surface in a turbulent flow*, Proceedings of the 27th AIAA Applied Aerodynamics Conference (2009).
78. H. Lienhart, M. Breuer and C. Köksoy, *Int. J. Heat Fluid Flow*, **29**, 783 (2008).
79. H. M. Kim, M. A. Moon and K. Y. Kim, *Energy*, **36**, 3419 (2011).
80. C. Silva, E. Marotta and L. Fletcher, *J. Electronic Packaging*, **129**, 157 (2006).
81. N. K. Burgess, M. M. Oliveira and P. M. Ligrani, *J. Heat Transfer*, **125**, 11 (2003).
82. A. Samad, K. D. Lee and K. Y. Kim, *Heat Mass Transfer*, **45**, 207 (2008).
83. S. M. Trujillo, B. David, B. Kenneth, T. Steven, B. David and B. Kenneth, *Turbulent boundary layer drag reduction using an oscillating wall*, 4th Shear Flow Control Conference (1997).
84. J. Fang, L. Lu and L. Shao, *Sci. in China Series G: Phys. Mech. and Astronomy*, **52**, 1233 (2009).
85. A. Baron and M. Quadrio, *Appl. Sci. Res.*, **55**, 311 (1996).
86. F. Laadhari, L. Skandaji and R. Morel, *Phys. Fluids*, **6**, 3218 (1994).
87. K. S. Choi, J. R. Debisschop and B. R. Clayton, *AIAA J.*, **36**, 1157 (1998).
88. K. S. Choi and B. R. Clayton, *Int. J. Heat Fluid Flow*, **22**, 1 (2001).
89. K. S. Choi, *Phys. Fluids*, **14**, 2530 (2002).
90. P. Ricco and M. Quadrio, *Int. J. Heat Fluid Flow*, **29**, 891 (2008).
91. W. J. Jung, N. Mangiavacchi and R. Akhavan, *Phys. Fluids A: Fluid Dynamics*, **4**, 1605 (1992).
92. M. Quadrio and P. Ricco, *J. Fluid Mech.*, **521**, 251 (2004).
93. K. S. Choi and M. Graham, *Phys. Fluids*, **10**, 7 (1998).
94. M. O. Kramer, *J. American Society for Naval Engineers*, **72**, 25 (1960).
95. F. W. Puryear, *Boundary layer control: Drag reduction by use of compliant coatings*, *David Taylor Model Basin Report No. 1668*, Naval Surface Warfare Center (1962).
96. C. R. Nisewanger, *Flow noise and drag measurements of vehicle with compliant coating*, *Report No. 8518 NOTS No. TP-3510*, US Naval Ordnance Test Station (1964).
97. H. Ritter and L. Messum, *Water tunnel measurements of turbulent skin friction on six different compliant surfaces of 1 ft length*, *Report No. ARL/N4/GHY/9/7, ARL/G/N9*, British Admiralty Research Laboratory (1964).
98. H. Ritter and J. Porteous, *Water tunnel measurements of skin friction on a compliant coating*, *Report No. ARL/N3/G/HY/9/7*, British Admiralty Research Laboratory (1964).
99. P. W. Carpenter and A. D. Garrad, *J. Fluid Mech.*, **155**, 465 (1985).
100. T. B. Benjamin, *J. Fluid Mech.*, **9**, 513 (1960).
101. R. Betchov, *J. Ship Res.*, **4**, 37 (1960).
102. M. T. Landahl, *J. Fluid Mech.*, **13**, 609 (1962).
103. V. M. Kulik, I. S. Poguda and B. N. Semenov, *Experimental investigation of one-layer viscoelastic coatings action on turbulent friction and wall pressure pulsations*, in *Recent Developments in Turbulence Management*, K. S. Choi Ed., Kluwer Academic Publishers, Dordrecht, Netherlands, 263 (1991).
104. B. N. Semenov, *On conditions of modelling and choice of viscoelastic coatings for drag reduction*, in *Recent Developments in Turbulence Management*, K. S. Choi Ed., Kluwer Academic Publishers, Dordrecht, Netherlands, 241 (1991).
105. K. S. Choi, X. Yang, B. R. Clayton, E. J. Glover, M. Atlar, B. N. Semenov and V. M. Kulik, *Proceedings of the Royal Society of London. Series A: Mathematical, Phys. Eng. Sci.*, **453**, 2229 (1997).
106. T. Endo and R. Himeno, *J. Turbulence*, **3**, 7 (2002).
107. S. Xu, D. Rempfer and J. Lumley, *J. Fluid Mech.*, **478**, 11 (2003).
108. T. Kawamura, Y. Moriguchi, H. Kato, A. Kakugawa and Y. Kodama, *Effect of bubble size on the microbubble drag reduction of a turbulent boundary layer*, ASME/JSME 2003 4th Joint Fluids Summer Engineering Conference (2003).
109. E. Afiza and H. Okanaga, *Effect of skin friction reduction by microbubbles in pipe flow*, Proceedings of the School of Engineering of Tokai University (2012).
110. Y. Kodama, A. Kakugawa, T. Takahashi and H. Kawashima, *Int. J. Heat Fluid Flow*, **21**, 582 (2000).
111. H. Kato, T. Iwashina, M. Miyanaga and H. Yamaguchi, *J. Marine*

Sci. Technol., **4**, 155 (1999).
112. M. E. McCormick and R. Bhattacharyya, *Naval Engineers J.*, **85**, 11 (1973).
113. C. L. Merkle and S. Deutsch, *Appl. Mech. Rev.*, **45**, 103 (1992).
114. N. K. Madavan, S. Deutsch and C. L. Merkle, *J. Fluids Eng.*, **107**, 370 (1985).
115. X. Lu, H. Kato and T. Kawamura, *Turbulent drag reduction effect by hydrogen and oxygen microbubbles made by electrolysis*, ASME 2006 2nd Joint US-European Fluids Engineering Summer Meeting Collocated With the 14th International Conference on Nuclear Engineering (2006).
116. S. J. Wu, C. H. Hsu and T. T. Lin, *Ocean Eng.*, **34**, 83 (2007).
117. J. Xu, M. R. Maxey and G. E. Karniadakis, *J. Fluid Mech.*, **468**, 271 (2002).
118. Y. Kodama, *Effect microbubbles distribution on skin friction reduction*, Proceedings of the International Symposium on Seawater Drag Reduction (1998).
119. S. J. Wu, K. Ouyang and S. W. Shiah, *Ocean Eng.*, **35**, 856 (2008).
120. F. Forrest and G. A. Grierson, *Paper Trade J.*, **92**, 39 (1931).
121. Z. J. You, J. Z. Lin, X. M. Shao and W. F. Zhang, *Chinese J. Chem. Eng.*, **12**, 319 (2004).
122. P. F. W. Lee and G. G. Duffy, *AIChE J.*, **22**, 750 (1976).
123. I. Radin, *Solid fluid drag reduction*, Ph.D. Thesis, University of Missouri - Rolla (1974).
124. I. Radin, J. L. Zakin and G. K. Patterson, *AIChE J.*, **21**, 358 (1975).
125. R. C. Vaseleski and A. B. Metzner, *AIChE J.*, **20**, 301 (1974).
126. A. L. Moyls and R. H. Sabersky, *Int. J. Heat Mass Transfer*, **21**, 7 (1978).
127. J. S. Paschkewitz, Y. V. Dubief, C. D. Dimitropoulos, E. S. G. Shaqfeh and P. Moin, *J. Fluid Mech.*, **518**, 281 (2004).
128. K. J. Mysels, Flow of thickened fluids, US Patent, 2,492,173 (1949).
129. Y. Wang, B. Yu, J. L. Zakin and H. Shi, *Adv. in Mech. Eng.*, **2011**, 1 (2011).
130. S. Tamano, M. Itoh, K. Kato and K. Yokota, *Phys. Fluids*, **22**, 055102 (2010).
131. I. Radin, J. L. Zakin and G. K. Patterson, *Exploratory drag reduction studies in non-polar soap systems*, in *Viscous Drag Reduction*, C. S. Wells Ed., Springer USA, 213 (1969).
132. J. Różański, *J. Non-Newtonian Fluid Mech.*, **166**, 279 (2011).
133. J. J. Wei, Y. Kawaguchi, F. C. Li, B. Yu, J. L. Zakin, D. J. Hart and Y. Zhang, *Int. J. Heat Mass Transfer*, **52**, 3547 (2009).
134. A. Krope and L. C. Lipus, *Appl. Therm. Eng.*, **30**, 833 (2010).
135. B. Yu and Y. Kawaguchi, *Int. J. Heat Fluid Flow*, **24**, 491 (2003).
136. B. Yu, F. Li and Y. Kawaguchi, *Int. J. Heat Fluid Flow*, **25**, 961 (2004).
137. H. W. Bewersdorff and D. Ohlendorf, *Colloid Polym. Sci.*, **266**, 941 (1988).
138. Y. Hu and E. Matthys, *Rheol. Acta*, **34**, 450 (1995).
139. C. Kim, S. R. Park, H. K. Yoon and J. R. Haw, *J. Chem. Eng. Jpn.*, **37**, 1326 (2004).
140. H. Zhang, D. Wang and H. Chen, *Arch. Appl. Mech.*, **79**, 773 (2009).
141. Y. Qi, Y. Kawaguchi, Z. Lin, M. Ewing, R. N. Christensen and J. L. Zakin, *Int. J. Heat Mass Transfer*, **44**, 1495 (2001).
142. L. Cheng, L. Liu and D. Mewes, *Drag reduction with surfactants and polymeric additives in multiphase flow*, in *Advances in Multiphase Flow and Heat Transfer*, L. Cheng and D. Mewes Eds., Bentham Science Publishers, USA, 149 (2012).
143. D. D. Kale and A. B. Metzner, *AIChE J.*, **22**, 669 (1976).
144. L. C. Chou, *Drag reducing cationic surfactant solutions for district heating and cooling systems*, Ph.D. Thesis, The Ohio State University (1991).
145. J. S. Lioumbas, A. A. Mouza and S. V. Paras, *Chem. Eng. Sci.*, **61**, 4605 (2006).
146. R. J. Wilkens and D. K. Thomas, *Int. J. Multiphase Flow*, **33**, 134 (2007).
147. D. Ohlendorf, W. Interthal and H. Hoffmann, *Rheol. Acta*, **25**, 468 (1986).
148. M. Hellsten, *J. Surfactants and Detergents*, **5**, 65 (2002).
149. R. C. Chang and J. L. Zakin, *Influence of polymer additives on velocity and temperature fields*, Proceedings of the IUTAM Symposium (1985).
150. S. H. Cho, C. S. Tae and M. Zaheeruddin, *Energy Convers. Manage.*, **48**, 913 (2007).
151. M. Hellsten and I. Harwigsson, *A new biodegradable friction reducing additive (FRA) for district cooling networks*, Proceedings of the 85th International District Heating and Cooling Association (IDHCA '94) (1994).
152. J. L. Zakin and H. L. Lui, *Chem. Eng. Commun.*, **23**, 77 (1983).
153. E. Suali, A. B. Hayder, Z. Hasan and M. Rahman, *J. Appl. Sci.*, **10**, 2683 (2010).
154. J. G. Savins, *Rheol. Acta*, **6**, 323 (1967).
155. J. L. Zakin, M. Brosh, A. Poreh and M. Warshavsky, *Chem. Eng. Professional Symposium Series*, **67**, 85 (1971).
156. A. Al-Sarkhi, *Int. J. Multiphase Flow*, **39**, 186 (2012).
157. A. Al-Sarkhi, E. Abu-Nada and M. Batayneh, *Int. J. Multiphase Flow*, **32**, 926 (2006).
158. A. Al-sarkhi, M. E. Nakla and W. H. Ahmed, *Int. J. Multiphase Flow*, **37**, 501 (2011).
159. M. Al-Yaari, A. Soleimani, B. Abu-Sharkh, U. Al-Mubaiyedh and A. Al-sarkhi, *Int. J. Multiphase Flow*, **35**, 516 (2009).
160. R. L. J. Fernandes, B. M. Jutte and M. G. Rodriguez, *Int. J. Multiphase Flow*, **30**, 1051 (2004).
161. N. Jia, M. Gourma and C. P. Thompson, *Chem. Eng. Sci.*, **66**, 4742 (2011).
162. D. Mowla and A. Naderi, *Chem. Eng. Sci.*, **61**, 1549 (2006).
163. J. Y. Xu, Y. X. Wu, H. Li, J. Guo and Y. Chang, *Chem. Eng. J.*, **147**, 235 (2009).
164. A. E. Green and R. S. Rivlin, *Quarterly of Appl. Mathematics*, **14**, 299 (1956).
165. J. A. Wheeler and E. H. Wissler, *Trans. Soc. Rheol.*, **10**, 353 (1966).
166. P. Townsend, K. Walters and W. M. Waterhouse, *J. Non-Newtonian Fluid Mech.*, **1**, 107 (1976).
167. B. Gervang and P. S. Larsen, *J. Non-Newtonian Fluid Mech.*, **39**, 217 (1991).
168. S. Gao, *Flow and heat transfer behavior of non-Newtonian fluids in rectangular ducts*, Ph.D. Thesis, University of Illinois at Chicago (1993).
169. C. Xie and J. P. Hartnett, *Ind. Eng. Chem. Res.*, **31**, 727 (1992).
170. B. K. Rao, *Heat transfer to viscoelastic fluids in a 5:1 rectangular duct*, Ph.D. Thesis, University of Illinois at Chicago (1988).
171. B. K. Rao, *Int. J. Heat Fluid Flow*, **10**, 334 (1989).

172. V. Bianco, O. Manca and S. Nardini, *Int. J. Therm. Sci.*, **50**, 341 (2011).
173. W. Duangthongsuk and S. Wongwises, *Int. J. Heat Mass Transfer*, **52**, 2059 (2009).
174. K. S. Hwang, S. P. Jang and S. U. S. Choi, *Int. J. Heat Mass Transfer*, **52**, 193 (2009).
175. D. Kim, Y. Kwon, Y. Cho, C. Li, S. Cheong, Y. Hwang, J. Lee, D. Hong and S. Moon, *Current Appl. Phys.*, **9**, 119 (2009).
176. P. Kumar and R. Ganesan, *Int. J. Civil and Environ. Eng.*, **6**, 385 (2012).
177. J. Lee, R. D. Flynn, K. E. Goodson and J. K. Eaton, *Convective heat transfer of nanofluids (DI water-Al2O3) in microchannels*, ASME-JSME Thermal Engineering Summer Heat Transfer Conference (2007).
178. S. E. B. Maïga, S. J. Palm, C. T. Nguyen, G. Roy and N. Galanis, *Int. J. Heat Fluid Flow*, **26**, 530 (2005).
179. U. Rea, T. McKrell, L. W. Hu and J. Buongiorno, *Int. J. Heat Mass Transfer*, **52**, 2042 (2009).
180. L. Syam Sundar, M. K. Singh and A. C. M. Sousa, *Int. Commun. Heat Mass Transfer*, **44**, 7 (2013).
181. R. S. Vajjha, D. K. Das and D. P. Kulkarni, *Int. J. Heat Mass Transfer*, **53**, 4607 (2010).
182. Z. S. Heris, S. G. Etemad and N. M. Esfahany, *Int. Commun. Heat Mass Transfer*, **33**, 529 (2006).
183. B. H. Chun, H. U. Kang and S. H. Kim, *Korean J. Chem. Eng.*, **25**, 966 (2008).
184. P. Samira, Z. H. Saeed, S. Motahare and K. Mostafa, *Korean J. Chem. Eng.*, **32**, 609 (2015).
185. Z. H. Liu and L. Liao, *Int. J. Therm. Sci.*, **49**, 2331 (2010).
186. M. Drzazga, A. Gierczycki, G. Dzido and M. Lemanowicz, *Chinese J. Chem. Eng.*, **21**, 104 (2013).
187. J. C. Yang, F. C. Li, W. W. Zhou, Y. R. He and B. C. Jiang, *Int. J. Heat Mass Transfer*, **55**, 3160 (2012).
188. F. C. Li, J. C. Yang, W. W. Zhou, Y. R. He, Y. M. Huang and B. C. Jiang, *Thermochim. Acta*, **556**, 47 (2013).
189. J. C. Yang, F. C. Li, Y. R. He, Y. M. Huang and B. C. Jiang, *Int. J. Heat Mass Transfer*, **62**, 303 (2013).
190. M. M. Kostic, *Critical issues and application potentials in nanofluids research*, ASME 2006 Multifunctional Nanocomposites International Conference (2006).
191. M. M. Kostic, *Critical issues in nanofluids research and application potentials* in *Nanofluids: Research, Development and Applications*, Y. Zhang Ed., Nova Science Pub. Inc., New York, USA, 1 (2013).
192. C. J. Walleck, *Development of steady-state, parallel-plate thermal conductivity apparatus for poly-nanofluids and comparative measurements with transient HWTC apparatus*, M.S. Thesis, Northern Illinois University (2009).
193. X. Wang, X. Xu and S. U. S. Choi, *J. Thermophys. Heat Transfer*, **13**, 474 (1999).
194. C. T. Nguyen, F. Desgranges, G. Roy, N. Galanis, T. Maré, S. Boucher and H. Angue Mintsa, *Int. J. Heat Fluid Flow*, **28**, 1492 (2007).
195. B. Aladag, S. Halelfadl, N. Doner, T. Maré, S. Duret and P. Estellé, *Appl. Energy*, **97**, 876 (2012).
196. P. Keblinski, J. A. Eastman and D. G. Cahill, *Mater. Today*, **8**, 36 (2005).
197. T. Maré, S. Halelfadl, O. Sow, P. Estellé, S. Duret and F. Bazantay, *Exp. Therm. Fluid Sci.*, **35**, 1535 (2011).